Research Square

Preprints are preliminary reports that have not undergone peer review.
They should not be considered conclusive, used to inform clinical practice,
or referenced by the media as validated information.

Temporal profiling of circulating plasma microRNAs during early experimental ovine fasciolosis using absolute RT-qPCR quantification

Diana M. Barrero Torres
University of Córdoba
Guillem Herrera Torres
University of Córdoba
José Pérez
University of Córdoba
Paula V. Huertas Abril
University of Córdoba
Nieves Abril
University of Córdoba
Pablo J. Rufino Moya
University of Córdoba
Leandro Buffoni
University of Córdoba
Magnlia Conde Felipe
University of Córdoba
Álvaro Martínez Moreno
University of Córdoba
M. Teresa Ruiz Campillo
v42rucam@uco.es
University of Córdoba
Verónica Molina Hernández
University of Córdoba

Research Article

Keywords: Fasciola hepatica, circulating microRNAs, miRNAs, absolute quantification, RT-qPCR, early infection, host-parasite interaction, zoonosis

Posted Date: November 25th, 2026

DOI: https://doi.org/10.21203/rs.3.rs-11761762/v1

License: This work is licensed under a Creative Commons Attribution 4.0 International License.
Read Full License

Additional Declarations: No competing interests reported.

Abstract

Fasciola hepatica (*F. hepatica*) is a trematode of major veterinary and zoonotic importance, causing hepatic damage and production losses. Early host–parasite interactions remain poorly characterized at the systemic molecular level. Circulating microRNAs (miRNAs) may provide valuable biomarkers of infection. This study investigated temporal changes in circulating host-derived miRNAs in experimentally infected sheep using absolute RT-qPCR quantification. Plasma samples from infected sheep and non-infected controls were collected at 1, 3, 9 and 17 days post-infection (dpi). The absolute abundance of 11 miRNAs was determined using standard curves, and temporal changes and correlations were assessed using non-parametric tests and Spearman correlation, with Benjamini–Hochberg correction. Infection induced early, temporally distinct changes in circulating miRNA abundance. Oar-miR-122 showed the earliest significant increase, reaching approximately sevenfold at 1 dpi. At 3 dpi, oar-miR-150 increased approximately ninefold, alongside significant elevations in oar-let-7g, oar-miR-133-5p and oar-miR-3957-3p. The latter remained significantly elevated until 9 dpi. Correlation analysis identified 32 significant associations, predominantly positive, revealing a cluster of interconnected miRNAs alongside distinct patterns for oar-miR-122 and oar-miR-3957-3p. Overall, early *F. hepatica* infection induces rapid and temporally distinct alterations in circulating miRNA profiles. Oar-miR-122, oar-miR-150, oar-let-7g and oar-miR-3957-3p emerge as promising candidates for further investigation as early biomarkers of fasciolosis. Absolute quantification provides a reproducible framework for their future validation.

Introduction

Fasciolosis, primarily caused by *Fasciola hepatica (F. hepatica)*, remains one of the most significant helminth infections in veterinary medicine owing to its widespread distribution, persistence within livestock production systems, and sustained impact on the health and productivity of food-producing animals, including cattle, sheep, and goats [1, 2]. Its veterinary importance stems from the progressive hepatic damage it induces, accompanied by weight loss and reduced milk yield, even in settings where anthelmintic treatments are available, highlighting the ongoing challenges associated with effective disease control [3, 4]. These health consequences translate into substantial economic losses, with annual costs reaching millions of dollars due to liver condemnation, decreased production efficiency, and expenditures related to parasite control and treatment programs. These health consequences translate into substantial economic losses, with annual costs reaching millions of dollars due to liver condemnation, decreased production efficiency, and expenditures related to parasite control and treatment programs. Importantly, fasciolosis also represents a relevant zoonotic disease, with human infections reported across multiple endemic regions worldwide, highlighting the interconnected health burden shared by livestock, humans, and the environment [1]. The zoonotic implications of the disease further underscore the need to strengthen integrated surveillance and management strategies within a One Health framework [4–6].

Advances in molecular approaches and experimental models have revealed that the successful establishment of *F. hepatica* relies on a highly dynamic and specialized host-parasite interaction initiated

within hours of infection. During this process, newly excysted juveniles (NEJs) deploy a range of mechanisms associated with tissue adhesion, migration, immune evasion, and cellular modulation, enabling them to penetrate the intestinal barrier and secure survival within the host [7–9].

Despite the pivotal role of these early events in disease pathogenesis and progression, the molecular and cellular mechanisms governing the dialogue between the parasite and host tissues during the initial stages of infection remain incompletely understood. This knowledge gap represents one of the major unresolved questions in fasciolosis biology and continues to hinder the development of early diagnostic tools as well as novel preventive and vaccine-based interventions targeting juvenile parasite stages [10–12].

microRNAs (miRNAs) are a class of small non-coding RNAs that regulate gene expression at the post-transcriptional level through the degradation or translational repression of specific messenger RNAs (mRNAs), thereby playing essential roles in a wide range of physiological and pathological processes [13, 14]. miRNAs can be released into the extracellular environment and circulate within a variety of biological fluids, where they contribute to molecular communication between cells and even across species [14]. In infectious diseases, miRNAs are increasingly recognized as key mediators of host-pathogen interactions, influencing processes related to pathogenesis, immune evasion, and infection establishment [15]. Moreover, the identification of altered circulating miRNAs signatures in viral, bacterial, and parasitic infections has generated considerable interest in their potential utility as minimally invasive biomarkers for disease diagnosis, clinical stratification and monitoring [16, 17].

The growing interest in extracellular miRNAs is partly attributable to their remarkable stability in circulation, which arises from their association with extracellular vesicles (EVs), lipoproteins, and protein complexes that protect them from degradation [18, 19]. This stability facilitates their reliable detection in clinical samples and supports their promise as diagnostic tools. Nevertheless, important challenges remain, particularly regarding methodological standardization and the clinical validation of reported findings [16, 20].

In parasitic infections, accumulating evidence suggests that extracellular miRNAs not only reflect disease status but also actively contribute to host-parasite communication [21]. Helminths release miRNAs associated with EVs that can modulate host immune responses and promote long-term parasite survival [22–24]. In addition, temporal changes in circulating and vesicle-associated miRNAs profiles throughout the course of infection suggest their potential value for tracking the biological dynamics of host-parasite interactions [25, 26]. Nonetheless, further evidence is required to fully define the role of these molecules as functional mediators and to establish their translational potential as clinically applicable biomarkers [21, 27].

Most previous circulating miRNAs studies in parasitology and extracellular RNA biology have relied predominantly on relative RT-qPCR quantification approaches based on endogenous normalization controls. Although widely used, relative quantification strategies remain strongly influenced by normalization selection, amplification variability, and the lack of universally stable endogenous reference

molecules in plasma and other biofluids. This issue is particularly relevant in inflammatory and infectious conditions, where systemic molecular remodelling may substantially alter the abundance of commonly used circulating reference miRNAs [28, 29]. Consequently, biologically relevant extracellular RNA alterations may be underestimated or distorted by normalization-associated variability.

Absolute quantification strategies offer an alternative analytical framework capable of directly estimating extracellular miRNAs abundance independently of endogenous normalization controls. By expressing transcript abundance as absolute molecule numbers relative to RNA input, absolute quantification may facilitate biological interpretation, improve inter-study comparability, and enable more precise evaluation of temporal extracellular RNA dynamics during rapidly evolving pathological processes. Despite these advantages, absolute circulating miRNAs quantification remains relatively underutilized in helminth infection research and has rarely been applied to experimental fasciolosis.

In the present study, we performed a time-course characterization of circulating miRNAs dynamics during early stages of experimental *F. hepatica* infection in sheep using an absolute RT-qPCR quantification strategy. The selected circulating miRNAs panel comprised host-derived extracellular miRNAs with established immunoregulatory functions and liver-associated relevance. By integrating temporal plasma profiling, analytical validation, and correlation analyses, the study aimed to characterize infection-associated extracellular RNA modulation patterns occurring during early parasite establishment. Exploratory comparative analyses with previously published hepatic immune-associated transcriptional datasets were additionally performed to evaluate potential temporal convergence between circulating extracellular RNA dynamics and hepatic immune responses during early fasciolosis.

Materials and Methods

Study Design and Sample Collection

Thirty six-month-old male Merino sheep were used in this study. Animals were sourced from a privately owned flock certified free of fasciolosis, and informed consent was obtained from the owners prior to enrolment. Sheep were maintained at the experimental farm of the University of Córdoba, where monthly faecal sedimentation examinations were performed to confirm the absence of *F. hepatica* and other parasitic infections. The study followed a cross-sectional experimental design (Fig. 1). Animals were randomly allocated to groups of six according to sampling time point. Age and body weight remained essentially uniform across groups (n = 30), as the interval between consecutive sampling points was less than eight days. Six animals were assigned to an uninfected control group (UC), whereas the remaining twenty-four sheep were orally challenged with 150 *F. hepatica* metacercariae (Italian strain; Ridgeway Research Ltd, UK).

Blood samples from infected and control animals were collected by jugular venipuncture into 10 mL EDTA Vacutainer® tubes (BD, Becton Dickinson, Franklin Lakes, NJ, USA). Infected sheep were sampled in groups of six at 1, 3, 9, and 17 days post-infection (dpi), representing the earliest stages of parasite

establishment [12, 30]. Under sterile conditions within a laminar-flow cabinet, 30 mL of whole blood from each animal was transferred to Corning® Falcon® polypropylene conical tubes and centrifuged at 2000 × g for 20 min at 4°C. This procedure yielded approximately 15 mL of plasma per sample. Recovered plasma was divided into ten 1.5 mL aliquots and stored at -80°C until miRNA isolation (Fig. 1).

All experimental procedures were approved by the Bioethics Committee of the University of Córdoba (approval number 2021PI/22) and conducted in accordance with European legislation governing the use of animals in research (Directive 2010/63/EU and Decision 2020/569/EU), as well as the corresponding Spanish regulations (Law 32/2007 and Royal Decree 1386/2018).

The biological samples and experimental animals analysed in the present study were previously included in an independent study focused on the identification and validation of endogenous reference miRNAs for relative RT-qPCR normalization during early ovine fasciolosis [31]. In contrast, the present work addresses a distinct scientific objective by investigating the temporal dynamics and biological relevance of circulating miRNAs using an absolute quantification strategy that does not rely on endogenous normalization controls, an approach that may reduce bias associated with reference gene variability in plasma miRNA studies [29].

Assessment of Plasma Haemolysis

To evaluate potential pre-analytical bias associated with haemolysis, free haemoglobin levels were quantified in all plasma samples prior to miRNA analysis. Haemolysis was assessed spectrophotometrically by measuring absorbance at 414 nm (A_{414}), corresponding to the haemoglobin Soret band, using a NanoDrop™ spectrophotometer (Thermo Fisher Scientific, Waltham, MA, USA). Each sample was analysed in four technical replicates, and mean absorbance values were calculated.

All plasma samples showed A_{414} values below 0.20, indicating minimal erythrocyte lysis and confirming their suitability for circulating miRNA analysis according to established recommendations for plasma-based miRNA studies [32, 33]. Therefore, no samples were excluded on the basis of haemolysis. Detailed haemolysis measurements for the biological samples included in the present study were previously reported as supplementary data in an independent study focused on endogenous reference miRNA validation during ovine fasciolosis [31].

Plasma RNA Extraction

Total RNA enriched for small RNAs was extracted from 600 µL of plasma using the miRNeasy Serum/Plasma Advanced Kit (Qiagen, Hilden, Germany) according to the manufacturer's instructions, with minor modifications optimized for low-input plasma samples. Briefly, plasma samples were thawed on ice and lysed using Buffer RPL to disrupt EVs and release circulating RNA species. Protein precipitation was subsequently performed using Buffer RPP, followed by centrifugation to remove insoluble material. The resulting supernatant was mixed with isopropanol and purified using silica

membrane-based RNeasy UCP MinElute spin columns (Qiagen, Hilden, Germany) according to the manufacturer's protocol. RNA was eluted in 20 µL of RNase-free water and stored at -80°C until reverse transcription. Carrier RNA was not added during extraction in order to avoid interference with downstream spectrophotometric quantification and to preserve the endogenous circulating miRNA profile.

RNA concentration and purity were assessed using a NanoDrop™ spectrophotometer (Thermo Fisher Scientific, Waltham, MA, USA). As an additional technical quality control, a subset of samples was analysed using a Hellma TrayCell microvolume system (Hellma GmbH & Co. KG, Müllheim, Germany), yielding comparable measurements. Spectrophotometric measurements were used to evaluate RNA purity and assess potential protein or residual organic contamination prior to downstream analyses. Because UV-Vis spectrophotometry may overestimate RNA concentration in low-input plasma samples due to the presence of residual contaminants, a conservative standardization strategy was applied prior to reverse transcription. RNA samples were adjusted to a nominal concentration of 5 ng/µL to maintain a consistent input volume-to-eluate ratio across samples and minimize technical variability during downstream RT-qPCR analyses [29, 33].

Reverse Transcription (RT) and Spike-in Control

Reverse transcription was performed using the miRCURY® LNA RT Kit (Qiagen, Hilden, Germany) according to the manufacturer's instructions. Each reaction contained 20 ng of RNA in a final volume of 20 µL. To monitor reverse transcription efficiency and assess potential technical variability, the synthetic RNA spike-in UniSp6 (Qiagen, Hilden, Germany) was added to the reverse transcription master mix following the manufacturer's recommendations. Because UniSp6 was introduced at the reverse transcription step, it served exclusively as a control for cDNA synthesis and downstream qPCR amplification and did not account for variability in RNA extraction.

Reverse transcription reactions were performed in a C1000 Touch Thermal Cycler (Bio-Rad, Hercules, CA, USA) under the following conditions: 37°C for 1 h and 45 min, followed by enzyme inactivation at 95°C for 5 min. Resulting cDNA samples were diluted 1:10 with nuclease-free water and stored at -80°C until quantitative PCR analysis.

Quantitative Real-Time PCR (RT-qPCR)

Quantitative real-time PCR (RT-qPCR) was performed using the miRCURY LNA miRNA PCR Assay (Qiagen, Hilden, Germany) on a MyiQ2 Real-Time PCR Detection System (Bio-Rad, Hercules, CA, USA), following the manufacturer's recommendations. Each qPCR reaction was prepared in a final volume of 10 µL containing diluted cDNA (0.3 ng/rx), miRNA-specific LNA primers, and SYBR Green master mix supplied with the assay system. All biological samples were analysed in technical triplicates for each miRNA target. To monitor potential contamination and nonspecific amplification, no-template controls

(NTCs) were included in every qPCR plate. Melting curve analyses were routinely performed to confirm amplification specificity across all analysed targets. Details of the miRNA assays used in the study, including assay identifiers and amplification efficiencies, are provided in Supplementary Table S1.

Threshold cycle (Ct) values were automatically determined using a uniform fluorescence threshold across all qPCR experiments. An inter-plate calibrator was included in every amplification run to control for inter-run variability and ensure analytical consistency across plates. Analytical reproducibility was additionally evaluated using the coefficient of variation (CV) among technical replicates.

All qPCR experiments and data reporting procedures were conducted in accordance with the Minimum Information for Publication of Quantitative Real-Time PCR Experiments (MIQE) guidelines [34, 35].

Standard Curve Generation and Absolute miRNA Quantification

Absolute quantification of circulating miRNAs was performed using a standard curve generated from serial dilutions of a synthetic RNA standard. For this purpose, synthetic cel-miR-39 RNA provided in the miRNA (cel-miR-39) Spike-In Kit (Norgen Biotek, Thorold, ON, Canada) was used. A stock solution was prepared by diluting 10 pmol of cel-miR-39 RNA in 300 µL of nuclease-free water. Reverse transcription was performed using 480 pg of RNA in a final reaction volume of 20 µL under the same conditions used for experimental samples.

A series of ten-fold serial dilutions of the resulting cDNA was prepared to generate a standard curve covering a dynamic range from 10^2 to 10^8 molecules per reaction. These standards were amplified by RT-qPCR using cel-miR-39-specific primers under the same conditions applied to target miRNAs. Standard curve amplification was performed in parallel with experimental samples to ensure consistency across runs. Ct values obtained from the dilution series were plotted against the logarithm of the corresponding number of molecules to generate a linear regression model. The standard curve was described by the equation:

$$Ct = -a \log (X_0) + b$$

where: Ct= threshold cycle; a= slope of the standard curve; X_0= initial molecule number/well; b = y-intercept

The PCR amplification efficiency (E) was calculated from the slope of the standard curve using the equation:

$$E = 10^{-1/a} - 1$$

Yielding an amplification efficiency of approximately 99.7%, consistent with optimal RT-qPCR performance and MIQE recommendations [34].

Absolute miRNA copy numbers in plasma samples were determined by interpolating Ct values into the standard curve, enabling direct quantification of circulating miRNA abundance. This approach assumes comparable amplification efficiencies across the different miRNA assays, which was confirmed by preliminary validation experiments showing similar PCR efficiencies for all targets analysed.

Selection of the miRNA Panel

The panel of circulating miRNAs evaluated in this study (Table 1) was selected based on their biological relevance, previous evidence of involvement in host-parasite interactions, immune regulation, hepatic processes, their potential as extracellular biomarkers, and their prior detection in ovine plasma. The panel was designed to simultaneously assess host immunoregulatory responses, liver-associated molecular alterations, and exploratory regulatory pathways potentially involved during the early stages of experimental fasciolosis.

The core host-derived miRNAs included oar-miR-21, oar-miR-150, oar-miR-148a, and oar-miR-122. These miRNAs have been associated with immunoregulatory signalling, inflammatory modulation, lymphocyte activation, macrophage polarization, TGF-β-related pathways, hepatic homeostasis, and hepatocellular injury [36–39]. The ovine miRNA oar-miR-3957-3p was also included to explore potential host-specific responses during infection [40]. In addition, the conserved regulatory miRNA oar-let-7g was included based on its reported involvement in immune modulation and the maintenance of cellular homeostasis [41].

Additional miRNAs, including oar-miR-29a, hsa-miR-181a-5p, oar-miR-133-5p, bta-miR-191, and hsa-miR-26b, were included to explore potential associations with extracellular matrix remodelling, T-cell activation, tissue injury responses, cellular stress adaptation, and other host regulatory pathways that may be involved during infection [42–46].

The initial panel also included fhe-miR-71a, a conserved invertebrate miRNA present in *F. hepatica*, and fhe-miR-Novel-11-5p, a candidate miRNA sequence described in *F. hepatica* [40]. However, during quality-control assessment, both analytes exhibited distorted read profiles consistent with the potential presence of shorter isomiR variants. Because this possibility could preclude unambiguous assignment to the canonical sequences and compromise their accurate quantification, both miRNAs were excluded from subsequent analyses.

Overall, the final panel of 11 miRNAs enabled an integrated assessment of host immune regulation, liver-associated molecular responses, and exploratory circulating biomarkers during the early stages of experimental *F. hepatica* infection. miRNAs were classified into three categories according to their functional relevance and/or tissue association: **(A)** central host-derived immunoregulatory miRNAs, including oar-miR-21, oar-miR-150, oar-miR-148a, and oar-let-7g; **(B)** liver-associated and tissue-remodelling-associated miRNAs, including oar-miR-122, oar-miR-3957-3p, and oar-miR-29a; and **(C)**

additional host-derived regulatory miRNAs, including hsa-miR-181a-5p, hsa-miR-26b, oar-miR-133-5p, and bta-miR-191.

Table 1
Biological rationale for the selection of circulating miRNAs included in the study.

microRNA	Main biological processes	Potential relevance during early fasciolosis	Category	Representative references
Central host-derived immunoregulatory miRNAs				
oar-miR-21	Immunoregulation, TGF-β signalling, inflammatory control, Treg polarization	Early modulation of anti-inflammatory and regulatory pathways during parasite establishment	Core host-derived	[38]
oar-miR-150	Lymphocyte differentiation, adaptive immunity, B/T-cell maturation	Regulation of early Th1/Th2-associated immune responses during infection	Core host-derived	[36]
oar-miR-148a	Immune tolerance, cytokine regulation, macrophage responses	Helminth-associated immunomodulation and suppression of inflammatory signalling	Core host-derived	[39]
oar-let-7g	Immune modulation, inflammatory signalling, cellular homeostasis	Regulation of systemic inflammatory responses during infection	Core host-derived	[41]
Liver-associated and tissue-remodelling-associated miRNAs				
oar-miR-122	Hepatic homeostasis, lipid metabolism, hepatocellular injury	Biomarker of liver damage associated with juvenile parasite migration	Core host-derived	[37]
oar-miR-3957-3p	Species-specific regulatory responses	Potential ovine-specific biomarker of early infection	Core host-derived	[40]
oar-miR-29a	Extracellular matrix remodelling, fibrosis-associated pathways, TGF-β signalling	Potential regulation of early tissue remodelling and fibrogenic responses	Additional host-derived	[44]
Additional host-derived regulatory miRNAs				
hsa-miR-181a-5p	T-cell activation, immune sensitivity tuning, inflammatory regulation	Potential modulation of immune activation thresholds during infection	Additional host-derived	[43]
hsa-miR-26b	Cell proliferation, immune signalling regulation	Exploratory assessment of generalized host regulatory responses	Additional host-derived	[46]
oar-miR-133-5p	Cellular stress responses, tissue	Exploratory marker potentially associated	Additional host-derived	[42]

microRNA	Main biological processes	Potential relevance during early fasciolosis	Category	Representative references
	remodelling, muscle-associated signalling	with tissue injury responses		
bta-miR-191	Cellular homeostasis, stress adaptation, extracellular RNA stability	Candidate circulating microRNA associated with systemic inflammatory responses	Additional host-derived	[45]

The miRNAs designated with the prefixes *hsa* and *bta* correspond to sequences annotated in *Homo sapiens* and *Bos taurus*, respectively. These miRNAs were included in the analysis after confirming ≥ 97.0% sequence identity with their homologous *Ovis aries* miRNAs and were therefore considered conserved equivalents for biological interpretation in the ovine species.

Statistical Analysis

Statistical analyses were performed using GraphPad Prism version 10.2.3 (GraphPad Software, San Diego, CA, USA) and R Project for Statistical Computing version 4.5.0 (R Foundation for Statistical Computing, Vienna, Austria).

Absolute circulating miRNA abundance values were expressed as transcript molecules per pg of total RNA. For each biological sample, technical triplicates were averaged prior to statistical analysis, and the resulting mean value was considered a single biological replicate.

Data distribution was evaluated using the Shapiro-Wilk normality test. Because several datasets did not fulfil normality assumptions and sample sizes were limited, nonparametric statistical analyses were applied throughout the study. Data were presented as mean ± standard error of the mean (SEM) unless otherwise indicated.

Comparisons among experimental groups were performed using the Kruskal-Wallis test followed by Dunn's multiple-comparison post hoc test for pairwise comparisons against uninfected controls. Adjusted *P* values were calculated to correct for multiple testing. Differences were considered statistically significant at adjusted $P < 0.05$.

Correlation analyses between selected circulating miRNAs were performed using Spearman's rank correlation coefficient. Spearman correlation matrices, hierarchical clustering analyses, and heatmap visualizations were generated in R using the pheatmap package. For each visualization, colour scales, cut-off values, and row- and column-clustering parameters were defined according to the corresponding matrix.

Integrated temporal comparisons between circulating miRNA profiles and hepatic immune-associated mRNA datasets were performed descriptively using fold-change trajectory analyses and temporal association mapping. Because both datasets originated from independent experiments performed under

comparable but non-identical experimental conditions, these analyses were intended to evaluate coordinated biological trends and temporal relationships rather than direct individual-level statistical correlations.

Results

Circulating miRNAs were quantified in plasma samples collected from experimentally infected sheep at 1, 3, 9, and 17 dpi and compared with those from uninfected controls (Fig. 1) using an absolute RT-qPCR quantification workflow. The selected panel comprised ovine host-derived miRNAs implicated in immune regulation, liver-associated processes, and host-parasite interactions (Table 1). Prior to biological analyses, the analytical performance and technical reproducibility of the quantification workflow were thoroughly validated.

Analytical Validation of the Absolute RT-qPCR Workflow

The workflow used for the absolute quantification of circulating miRNAs met the established quality criteria for plasma-based RT-qPCR analysis, encompassing preanalytical sample quality, reverse transcription, and amplification performance. Haemolysis assessment based on the absorbance of the haemoglobin Soret band at 414 nm (A_{414}) revealed consistently low values across all samples, ranging from 0.06 to 0.19 among the experimental groups (Fig. 2A). All measurements remained below the commonly applied threshold of 0.2 for identifying haemolyzed samples in circulating miRNA studies [32], indicating no evidence of substantial haemolysis according to this criterion.

Spectrophotometric assessment of extracted RNA yielded A_{260}/A_{280} ratios close to 2.0 and A_{260}/A_{230} ratios generally exceeding 1.8, consistent with low levels of protein and organic compound contamination. Measurements obtained using the NanoDrop™ and Hellma TrayCell systems were comparable, indicating good agreement between the two platforms. Reverse transcription performance, assessed using the synthetic UniSp6 spike-in control, was also comparable across experimental groups, with no systematic variation suggestive of meaningful differences in reverse transcription efficiency (Fig. 2B). Detailed findings from the assessment of haemolysis, RNA quality, and UniSp6-based technical control in the same sample cohort have been reported previously in an independent study [31].

Absolute quantification was performed using an external standard curve generated from serial dilutions of synthetic cel-miR-39 RNA, spanning 10^2 to 10^8 molecules per reaction. The standard curve exhibited excellent linearity across the entire concentration range (Fig. 2C), with a regression equation of $y = -3.3296 \log(X_0) + 39.698$ and a coefficient of determination (R^2) of 0.9986. The calculated amplification efficiency was 99.7%, closely approaching the theoretical optimum and falling within the ranges recommended by the MIQE guidelines. Ct variability among technical triplicates remained within acceptable analytical limits, with coefficients of variation (CVs) below 5% for all miRNA assays evaluated (Supplementary Table S2), demonstrating high technical reproducibility. Melting curve analysis further

supported amplification specificity across all targets examined. In addition, amplification efficiencies were within acceptable ranges and were comparable across individual miRNA targets.

Immunoregulatory Host-Derived Circulating miRNAs During Early Fasciolosis

Temporal profiling of circulating host immunoregulatory miRNAs revealed changes in their abundance during the early stages of experimental *F. hepatica* infection, with the most pronounced alterations observed at 3 dpi (Fig. 3A; Table 2). Among the miRNAs examined, oar-miR-150 and oar-let-7g exhibited significant increases in circulating abundance compared with uninfected controls, whereas changes in oar-miR-148a and oar-miR-21 did not reach statistical significance.

The largest change was observed for oar-miR-150, which exhibited an approximately ninefold increase in circulating abundance at 3 dpi relative to uninfected controls (adjusted $P = 0.0007$). Although elevated levels persisted in several animals at 9 and 17 dpi, these differences were no longer statistically significant, with greater interindividual variability observed at both time points. Similarly, oar-let-7g showed a significant increase at 3 dpi (adjusted $P = 0.016$), followed by a decline towards baseline levels from 9 dpi onwards. Thus, both miRNAs displayed a marked early increase in circulating abundance, although their subsequent temporal profiles differed.

Table 2
Absolute abundance and temporal statistical analysis of circulating miRNAs during early experimental *F. hepatica* infection.

miRNA	Group	Mean molecules/pg total RNA	SEM	Fold change *vs* control	Adjusted *P vs* control
Core immunoregulatory host-derived miRNAs					
oar-miR-21	Control	229.47	26.57	1.00	—
	1-dpi	448.33	128.27	1.95	0.851
	3-dpi	314.35	56.54	1.37	> 0.999
	9-dpi	171.88	26.78	0.75	> 0.999
	17-dpi	138.92	36.09	0.61	0.674
oar-miR-150	Control	241.07	59.85	1.00	—
	1-dpi	368.22	100.82	1.53	> 0.999
	3-dpi	2272.87	258.05	9.43	***0.0007
	9-dpi	828.98	209.32	3.44	0.182
	17-dpi	592.95	252.83	2.46	> 0.999
oar-miR-148a	Control	92.35	22.85	1.00	—
	1-dpi	176.12	36.95	1.91	0.462
	3-dpi	244.12	54.03	2.64	0.132
	9-dpi	102.37	18.81	1.11	> 0.999
	17-dpi	89.73	32.17	0.97	> 0.999
oar-let-7g	Control	95.33	22.45	1.00	—
	1-dpi	162.78	34.05	1.71	0.9
	3-dpi	363.37	66.12	3.81	*0.016
	9-dpi	136.92	31.53	1.44	> 0.999
	17-dpi	94.02	35.40	0.99	> 0.999
Liver-associated and tissue-remodelling-associated miRNAs					
oar-miR-122	Control	8.60	3.02	1.00	—
	1-dpi	60.15	8.19	6.99	**0.0019
	3-dpi	30.55	17.38	3.55	> 0.999
	9-dpi	18.63	5.15	2.17	> 0.999

miRNA	Group	Mean molecules/pg total RNA	SEM	Fold change *vs* control	Adjusted *P vs* control
	17-dpi	23.25	4.94	2.70	0.615
oar-miR-3957-3p	Control	0.25	0.03	1.00	—
	1-dpi	0.22	0.06	0.87	> 0.999
	3-dpi	1.62	0.18	6.47	**0.0088
	9-dpi	1.52	0.49	6.07	*0.046
	17-dpi	0.28	0.06	1.13	> 0.999
oar-miR-29a	Control	67.02	27.95	1.00	—
	1-dpi	82.30	13.60	1.23	> 0.999
	3-dpi	151.32	32.23	2.26	0.095
	9-dpi	63.53	10.87	0.95	> 0.999
	17-dpi	61.05	22.28	0.91	> 0.999
Additional host regulatory miRNAs					
hsa-miR-181a-5p	Control	13.42	5.01	1.00	—
	1-dpi	23.98	6.19	1.79	0.432
	3-dpi	20.67	6.25	1.54	> 0.999
	9-dpi	8.22	1.68	0.61	> 0.999
	17-dpi	4.23	0.74	0.32	0.168
hsa-miR-26b	Control	28.87	4.78	1.00	—
	1-dpi	59.08	15.93	2.05	0.34
	3-dpi	28.58	3.25	0.99	> 0.999
	9-dpi	21.42	2.38	0.74	> 0.999
	17-dpi	15.30	3.41	0.53	0.295
oar-miR-133-5p	Control	1.90	0.42	1.00	—
	1-dpi	1.65	0.11	0.87	> 0.999
	3-dpi	18.48	5.18	9.73	*0.031
	9-dpi	7.27	5.59	3.82	> 0.999
	17-dpi	1.63	0.63	0.86	> 0.999

miRNA	Group	Mean molecules/pg total RNA	SEM	Fold change *vs* control	Adjusted *P vs* control
bta-miR-191	Control	176.02	47.05	1.00	—
	1-dpi	222.67	44.71	1.27	> 0.999
	3-dpi	398.77	62.26	2.27	0.095
	9-dpi	161.13	32.86	0.92	> 0.999
	17-dpi	98.58	25.79	0.56	> 0.999

Absolute expression levels are expressed as miRNA molecules per pg of total RNA. Data are presented as mean ± SEM for each experimental group. Fold changes were calculated relative to uninfected controls. Statistical comparisons were performed using Kruskal-Wallis analysis followed by Dunn's multiple-comparison post hoc test with Benjamini-Hochberg false discovery rate correction. Adjusted P values correspond to comparisons versus the control group at each experimental time point. Significant adjusted *P* values: ***adjusted P** < 0.05, ****adjusted P** < 0.01, and *****adjusted P** < 0.001 are highlighted in bold.

Likewise, oar-miR-148a exhibited a trend towards increased expression during the early stages of infection, particularly at 1 and 3 dpi, when several animals showed higher levels than those observed in the control group. This pattern was consistent with that observed for oar-miR-150 and oar-let-7g, despite the lack of statistically significant differences. At later time points (9 and 17 dpi), expression levels were generally comparable to those of the control group.

In contrast, oar-miR-21 exhibited a more heterogeneous expression profile, characterized by substantial inter-individual variability, particularly at 1 and 3 dpi. During this period, several animals displayed higher expression levels than controls, with the highest individual values recorded at 1 dpi. By 17 dpi, expression levels tended to decline relative to those observed during the early stages of infection. However, none of these changes reached statistical significance.

Liver-Associated and Ovine-Enriched Circulating miRNAs During Early Fasciolosis

Liver-associated and ovine-enriched miRNAs exhibited distinct expression patterns during the early stages of experimental *F. hepatica* infection (Fig. 3B; Table 2). The earliest significant change was detected in oar-miR-122, with circulating levels increasing approximately sevenfold at 1 dpi compared with uninfected controls (adjusted $P = 0.0019$). This represented the first statistically significant alteration detected in plasma. Even though mean oar-miR-122 levels remained elevated at subsequent time points, increased inter-animal variability was observed, and the differences were no longer statistically significant after correction for multiple comparisons. Notably, this early increase preceded the major elevations observed in several of the immunoregulatory miRNAs examined in this study.

In contrast, oar-miR-3957-3p exhibited a delayed response, with plasma levels increasing more than sixfold relative to controls at both 3 and 9 dpi (adjusted *P* = 0.0088 and 0.046, respectively), before returning to near-baseline levels by 17 dpi. Importantly, oar-miR-3957-3p was the only miRNA in this group to exhibit significant differences at two consecutive sampling time points and showed one of the largest relative increases, despite its low basal abundance in control animals. Accordingly, whereas oar-miR-122 responded predominantly at 1 dpi, the increase in oar-miR-3957-3p was more pronounced at later time points. oar-miR-29a showed a modest upward trend at 3 dpi, coinciding with the increases observed in other miRNAs within the panel. Nevertheless, this change did not reach statistical significance after correction for multiple comparisons, and its levels returned to near-baseline values at 9 and 17 dpi.

Additional Host-Derived Circulating miRNAs During Early Fasciolosis

Additional host-derived circulating miRNAs exhibited heterogeneous patterns of temporal regulation during experimental *F. hepatica* infection (Fig. 3C; Table 2). Of these, oar-miR-133-5p showed a significant increase at 3 dpi (adjusted *P* = 0.031), followed by a return to baseline levels at subsequent time points. The increase in oar-miR-133-5p was transient and accompanied by substantial inter-individual variability among infected animals.

The remaining miRNAs displayed distinct temporal trends, none of which reached statistical significance after correction for multiple comparisons. hsa-miR-181a-5p tended to exhibit higher circulating levels during the early stages of infection, followed by a progressive decline that was particularly evident at 17 dpi. Likewise, bta-miR-191 and hsa-miR-26b showed trends towards increased abundance at 3 and 1 dpi, respectively, with both exhibiting lower levels at 17 dpi. Nonetheless, these fluctuations did not follow a consistent pattern relative to uninfected controls (Supplementary Table S3).

Global Analysis of Associations Among Circulating miRNA Abundance Profiles During Early Experimental Fasciolosis

Spearman's rank correlation analysis was performed to characterize the relationships among the abundance profiles of the 11 circulating miRNAs quantified in infected animals (*n* = 24). Of the 55 possible pairwise comparisons, 32 (58.2%) remained statistically significant after Benjamini-Hochberg correction for multiple testing (FDR < 0.05; Fig. 4; Supplementary Figure S2; Supplementary Table S4). Because the analysis was conducted using pooled data across infection stages, these associations should be interpreted as patterns of covariation in circulating miRNA abundance rather than evidence of direct biological interactions between miRNAs.

Nearly all significant associations were positive (31/32; 96.9%), with correlation coefficients ranging from ρ = 0.487 to ρ = 0.920. Of these, 17 (54.8%) were strong (ρ ≥ 0.70), whereas the remaining associations were moderate in magnitude. The strongest correlations involved oar-let-7g, oar-miR-29a, oar-miR-148a, and bta-miR-191 (ρ = 0.87–0.92; adjusted P < 0.001), indicating a high degree of

concordance in their circulating abundance profiles (Fig. 4). In contrast, the only significant negative correlation was detected between oar-miR-122 and oar-miR-3957-3p and was moderate in magnitude ($\rho = -0.545$; adjusted $P < 0.005$).

Significant correlations were not uniformly distributed across miRNAs but were predominantly concentrated among a subset of highly connected miRNAs (Fig. 4; Supplementary Table S4). bta-miR-191, oar-let-7g, and oar-miR-148a exhibited the highest number of significant associations, each showing eight positive correlations, followed by oar-miR-29a with seven. oar-miR-21, hsa-miR-181a-5p, oar-miR-133-5p, and oar-miR-150 each displayed six significant positive correlations, whereas hsa-miR-26b exhibited five.

Correlation strength also varied among these highly connected miRNAs, independently of the number of significant associations. Notably, oar-miR-21 exhibited six significant correlations, all of which were strong ($\rho \geq 0.70$), whereas five of the seven significant correlations involving oar-miR-29a were strong. In addition, bta-miR-191 and oar-let-7g each exhibited five strong correlations, followed by oar-miR-148a with four. Despite the greater connectivity of the latter miRNAs, oar-miR-21 and oar-miR-29a exhibited the highest mean correlation coefficients across the major network components (mean $\rho = 0.779$ and 0.775, respectively) (Fig. 4; Supplementary Table S4).

Conversely, oar-miR-3957-3p and, particularly, oar-miR-122 exhibited fewer significant associations and occupied more peripheral positions within the network. oar-miR-3957-3p showed three significant associations, comprising two moderately positive correlations and one negative correlation. In comparison, oar-miR-122 displayed only one significant association, corresponding to its inverse relationship with oar-miR-3957-3p. The high abundance of oar-miR-122 at 1 dpi, coupled with its limited connectivity, was consistent with a temporal abundance profile distinct from that of miRNAs predominantly involved in positive associations. By comparison, oar-miR-3957-3p retained some connectivity with the main network cluster through its two positive associations, while also contributing to the only significant negative correlation identified in the network (Fig. 4; Supplementary Table S4). These findings indicate that, over the experimental period, the circulating abundance of most miRNAs examined exhibited significant positive covariation, although a subset displayed distinct patterns of association.

Temporal Comparison of Circulating miRNAs and Hepatic Immune Mediators

The temporal dynamics of circulating miRNAs were compared with the expression profiles of hepatic mediators involved in immune responses previously reported by Ruiz-Campillo et al. (2023) [30] (Fig. 5A-C; Supplementary Table S5; Supplementary Figure S3). Circulating miRNAs were assessed at 1, 3, 9, and 17 dpi, while hepatic transcript expression was evaluated at 4, 8, and 16 dpi. Despite being conducted under comparable experimental conditions, the two studies involved different animals and did not share identical sampling time points. Accordingly, the comparison was restricted to characterizing temporal

patterns in both datasets, without inferring direct correlations between circulating miRNA levels and hepatic transcript expression.

Changes in circulating miRNA abundance were primarily observed during the early stages of infection, while the most pronounced increases in hepatic immune mediator expression occurred at later time points. Specifically, oar-miR-150 and oar-let-7g reached peak levels at 3 dpi, preceding the increased hepatic expression of IL-10, TGF-β, and FOXP3 during the intermediate and late stages of infection (Fig. 5A; Supplementary Figure S3). Among these miRNAs, oar-miR-150 exhibited a particularly pronounced early increase followed by a gradual decline, with levels remaining above baseline through 17 dpi. Over this period, hepatic IL-10 and TGF-β expression also increased, accompanied by a more modest increase in FOXP3 expression.

A comparable pattern was observed for oar-miR-21 and oar-miR-148a, both of which tended to increase during the first days of infection, without reaching statistical significance relative to controls. These early trends preceded the later increases in hepatic IL-10 and TGF-β expression in the case of oar-miR-21, and FOXP3 expression in the case of oar-miR-148a (Fig. 5A-C). oar-miR-122, by contrast, displayed a distinct temporal pattern, characterized by a marked increase at 1 dpi, while hepatic TNF-α and IL-1β expression increased primarily at 8 and 16 dpi (Figs. 3B and 5A). The higher abundance of oar-miR-3957-3p observed at 3 and 9 dpi also preceded the peak in hepatic IL-4 expression at 16 dpi (Fig. 5B). IFN-γ exhibited less pronounced changes, with increased hepatic expression at 16 dpi. Nevertheless, as these data were obtained from independent studies, the observed temporal similarities do not establish direct correlations or provide evidence that circulating miRNAs regulate hepatic immune mediator expression.

Discussion

In this study, we characterized the temporal dynamics of a panel of circulating host miRNAs during the early stages of experimental *F. hepatica* infection in sheep using absolute quantification by RT-qPCR. A major challenge in biofluid miRNA analysis is the lack of sufficiently stable endogenous reference controls [29, 45], particularly during infectious and inflammatory processes, when systemic changes may alter the abundance of miRNAs commonly used for normalization [47]. To address this limitation, we adopted an absolute quantification approach based on external standard curves, following the MIQE guidelines [34, 35]. The procedure incorporated haemolysis and RNA quality assessments, the UniSp6 spike-in control, triplicate reactions, and correction for multiple comparisons [48]. This approach enabled miRNA abundance to be estimated independently of endogenous reference miRNAs, without entirely eliminating variability associated with sample processing and the different analytical steps. Expressing miRNA abundance on an absolute scale also facilitates the interpretation of observed changes and may improve comparability across studies, provided that analytical procedures are adequately harmonized [28].

Our findings revealed alterations in circulating miRNA levels as early as the first day following *F. hepatica* infection. The earliest response was observed for oar-miR-122, which increased approximately sevenfold

relative to uninfected controls at 1 dpi. This miRNA is highly abundant in mature hepatocytes and plays an important role in lipid metabolism and the maintenance of hepatocellular identity [37, 49]. Circulating miR-122 levels rise rapidly in response to various forms of liver injury and, under certain conditions, may increase earlier and to a greater extent than conventional serum transaminases [50, 51]. Accordingly, miR-122 has been proposed as a biomarker of subclinical hepatocellular injury [52]. During fasciolosis, the migration of juvenile flukes through the hepatic parenchyma causes traumatic lesions, focal haemorrhage, and necrosis [53]. These processes also involve parasite-derived molecules that facilitate host tissue degradation, including cathepsins and saponins [10, 54]. The increase in oar-miR-122 at 1 dpi may reflect early infection-associated disturbances, although its occurrence at such an early stage, when juvenile flukes are still in the initial phases of migration, makes it difficult to attribute this response directly to hepatic parenchymal damage. The rapidity of this response is noteworthy, particularly because it precedes the major hepatic transcriptomic changes reported from 4–8 dpi onwards [30, 55]. Interindividual differences in baseline miR-122 abundance, potentially influenced by genetic, hormonal, and metabolic factors [56], may also partly account for the greater variability observed from 3 dpi onwards.

In contrast, oar-miR-3957-3p exhibited a more sustained response, with levels exceeding those of uninfected controls by more than sixfold at both 3 and 9 dpi. Its biological function remains poorly characterized, but its complementary strand has been identified among the differentially expressed serum miRNAs in *F. hepatica*-infected sheep during the hepatic phase of infection [40]. An interaction with DOCK1, a gene involved in myoblast fusion, has also been predicted [57], although the relevance of this putative interaction to fasciolosis remains unknown. By comparison, oar-miR-29a showed only a nonsignificant upward trend at 3 dpi. Previous studies in models of liver disease have shown that certain circulating miRNAs may reflect hepatocellular stress and tissue remodelling [58], without providing sufficient evidence to attribute the changes observed here directly to these processes. The distinct temporal profiles of oar-miR-122, characterized by an early increase, and oar-miR-3957-3p, which exhibited a more sustained elevation, suggest that these miRNAs may provide complementary information during the initial stages of infection. This possibility is particularly relevant given the limitations of coprological and serological diagnostic methods during this period [40, 53]. Establishing their potential diagnostic value will require validation in independent studies designed to assess their specificity, reproducibility, and ability to discriminate between infected and uninfected animals.

Among the immune-related miRNAs examined, oar-miR-150 and oar-let-7g exhibited significant changes at 3 dpi. miR-150 is predominantly expressed in mature B and T lymphocytes, where it contributes to B-cell precursor proliferation, CD4 + T-cell differentiation, and IL-2 production [59, 60]. Intracellular miR-150 expression has also been reported to decrease following antigenic activation [61]. In the present study, plasma oar-miR-150 levels increased approximately ninefold at 3 dpi before progressively declining. This pattern may reflect early changes in lymphocyte activation or population distribution, consistent with the immune reorganization previously described in sheep infected with *F. hepatica* [62]. Differential expression of miR-150-5p has also been reported in mice infected with *F. gigantica* [63], providing a precedent for its potential involvement in host responses to liver flukes. Differences in host and parasite

species, together with the distinct biological samples analysed, preclude direct comparisons with the plasma changes observed here. The alteration in oar-let-7g at 3 dpi is also of interest given the immunoregulatory functions attributed to the let-7 family, including its involvement in Toll-like receptor signalling and T-helper cell polarization [65]. Several members of this family have also been identified in helminth-derived EVs, suggesting a potential role in parasite-host communication [65]. These previous findings may inform the interpretation of the observed changes in oar-let-7g, but its cellular origin and potential immunomodulatory role during infection remain unknown. Similarly, oar-miR-148a, which has been implicated in B-cell tolerance and Th1-cell survival [39, 66], exhibited a temporal profile similar to that of oar-miR-150, although changes in its circulating levels did not reach statistical significance. Meanwhile, oar-miR-21 showed marked interindividual variability, potentially reflecting differences in inflammatory responses among animals. This interpretation is consistent with the immune heterogeneity and altered macrophage polarization reported during acute ovine fasciolosis [67, 68], as well as the regulatory functions attributed to miR-21 in various inflammatory processes [69–71]. A direct relationship between these processes and the observed variability in plasma miR-21 levels remains to be established. In addition, oar-miR-133-5p increased significantly at 3 dpi, with considerable interindividual variability and limited information available regarding its potential role during infection. Collectively, these profiles are consistent with the complexity of the early immune response to *F. hepatica*, in which Th1, Th2, and regulatory components coexist [30, 72], without allowing the cellular populations contributing to individual changes to be identified from plasma measurements alone.

Correlation analysis, restricted to samples from infected animals, revealed a marked predominance of positive associations (31 of 32), indicating that many circulating miRNAs exhibited similar patterns of variation within this group. Notably, the most highly connected miRNAs (bta-miR-191, oar-let-7g, oar-miR-148a, and oar-miR-29a) were not those showing the largest changes in abundance relative to uninfected controls. This data suggests that the magnitude of individual miRNA responses does not necessarily determine the strength or extent of their associations with other miRNAs. Among the most highly connected miRNAs, bta-miR-191 is of particular interest because of its involvement in the maintenance of regulatory T cells and CD8 + T cells through STAT5-related mechanisms [73], as well as its reported role in the HIF-1α/ZONAB/cyclin D1 axis in experimental models of hypoxia-associated liver injury [74]. These functions provide a biological rationale for further investigation, but the role of bta-miR-191 in fasciolosis has yet to be established. oar-miR-29a was notable for the strength of its correlations despite showing no significant changes in abundance relative to controls. The miR-29 family is involved in extracellular matrix regulation and hepatic stellate cell activation [75]. Its release in EVs has also been shown to influence its availability and antifibrotic activity [76], whereas miR-29 overexpression can modulate TLR2/TLR4 signalling and exert hepatoprotective effects in certain experimental models [77]. These findings provide relevant information for interpreting the associations involving oar-miR-29a, with any potential link to hepatic remodelling still requiring targeted investigation. Conversely, oar-miR-122 and oar-miR-3957-3p exhibited limited connectivity and formed the only negatively correlated miRNA pair, possibly reflecting their distinct temporal expression profiles. As correlation analyses were performed exclusively in infected animals, it remains unclear whether similar patterns also occur in

uninfected sheep. Shared time-dependent changes may also have contributed to some of the observed correlations. Accordingly, these observations should be interpreted as patterns of covariation among circulating miRNAs rather than evidence of direct regulatory interactions, a common cellular origin, or shared biological functions.

Finally, the major plasma miRNA alterations detected between 1 and 3 dpi preceded the changes in hepatic IFN-γ, IL-4, IL-10, and TGF-β expression reported between 4 and 16 dpi, as well as those in TNF-α and IL-1β between 8 and 16 dpi, in an independent study [30]. This temporal difference is of particular interest given the ability of *F. hepatica* to modulate host immune responses during the earliest stages of infection [78, 79]. Because circulating miRNAs originate from multiple tissues and cell populations, their plasma abundance may reflect biological disturbances that do not necessarily coincide with gene expression changes detected in the liver [28, 80]. The temporal and functional relationships between these observations remain to be established through analyses conducted in the same individuals, given that the available findings were obtained from independent studies involving different animals and sampling schedules.

Limitations and future perspectives

The findings of this study should be interpreted considering several limitations. First, the assessment of circulating miRNAs and hepatic responses in different animals precluded the establishment of direct relationships between these two compartments, and the observed correlations may reflect shared temporal patterns rather than direct biological associations. Furthermore, the small sample size, interindividual variability, and restriction of the analysis to eleven miRNAs may have limited the detection of additional relevant changes. The potential parasitic origin of some conserved sequences and the quantification of miRNAs in whole plasma, without distinguishing between their different carrier-associated forms, further complicate the determination of their origin and biological function (Boukouris & Mathivanan, 2015; Ljungström & Oltra, 2025). Finally, the lack of functional assays prevents definitive conclusions regarding the regulatory roles of the observed alterations during infection.

Despite these limitations, the study has several methodological strengths, including absolute quantification in accordance with MIQE guidelines, which avoids reliance on endogenous reference miRNAs that may exhibit variable stability in plasma [34, 35]. Standardized procedures, technical replicates, and correction for multiple comparisons further support the robustness of the findings. Moreover, the investigation of early infection stages enabled the detection of changes in specific circulating miRNAs as early as one day post-infection, before a detectable serological response. Nevertheless, further research is required to establish whether these changes are infection-specific and to assess their potential utility as diagnostic biomarkers.

Future studies should assess circulating miRNAs and hepatic responses in the same animals, validate the findings for oar-miR-122 and oar-miR-3957-3p in independent groups, and investigate their circulating carrier-associated forms and potential parasitic origin. Integrating multi-omics approaches

with functional assays would also help clarify the biological significance of these alterations and their relevance during the early stages of *F. hepatica* infection.

Conclusions

Experimental infection with *F. hepatica* induced early changes in circulating host miRNA levels in sheep, with distinct expression patterns throughout the course of infection. Among the most notable findings was an approximately sevenfold increase in oar-miR-122 levels at 1 dpi, potentially reflecting early hepatic alterations. At 3 dpi, increased levels of oar-miR-150 and oar-let-7g were detected, possibly associated with the host immune response, whereas oar-miR-3957-3p remained elevated from 3 to 9 dpi. These changes preceded both the hepatic immune responses reported in previous studies and the time points at which infection typically becomes detectable using coprological and serological methods. Correlation analysis revealed a predominance of positive associations among the miRNAs investigated, with bta-miR-191, oar-let-7g, and oar-miR-148a exhibiting the highest numbers of correlations, while oar-miR-21 and oar-miR-29a showed the strongest associations. In contrast, oar-miR-122 and oar-miR-3957-3p displayed distinct correlation patterns. Although these findings suggest associations among the expression profiles of certain miRNAs, they do not establish direct regulatory relationships. From a methodological perspective, absolute quantification enabled the assessment of these changes without reliance on endogenous reference miRNAs, whose expression may be unstable during infection.

Collectively, these findings identify oar-miR-122 and oar-miR-3957-3p as potential candidate biomarkers for the early detection of *F. hepatica* infection in sheep. However, their diagnostic utility requires validation in independent animal groups to assess their ability to discriminate between infected and uninfected animals. Further investigations integrating paired plasma and tissue analyses, sequencing approaches, and functional studies are also warranted to elucidate their tissue origin and biological significance.

Declarations

Ethics approval and consent to participate

This experiment was approved by the Bioethics Committee of the University of Córdoba (code no. 2021PI/22) which complied with European (2010/63/EU, Decision 2020/569/EU) and Spanish (L32/2007 and RD 1386/2018) guidelines on animal experimentation. The owner of the private ovine farm authorizes the use of the animals for research purposes.

Consent for publication

Not applicable.

Availability of data and materials

The datasets generated and/or analysed during the current study are available from the corresponding author upon reasonable request.

Competing interests

Not applicable.

Funding

José Pérez and Álvaro Martínez-Moreno acknowledge funding received from project PERSEUS (PID2023–152150OB-C22) and Verónica Molina-Hernández acknowledges the financial support received from project INTERACTOMVAC (CNS2022-135144); both funded by the Spanish Ministry of Science and Innovation.

Authors' contributions

Diana M. Barrero-Torres and Guillem Herrera-Torres: Performed the analysis and wrote the paper.

Paula V. Huertas-Abril, Nieves Abril, M. Teresa Ruiz-Campillo, José Pérez and Verónica Molina-Hernández: Conceived and designed the analysis; contributed data and analysis tools.

Pablo J. Rufino-Moya, Leandro Buffoni, Magnolia Conde-Felipe and Álvaro Martínez-Moreno: Collected the data and the samples.

Acknowledgements

All schematic representations were created with BioRender.com, Medical smart art and/or Canva.

References

1. Mas-Coma, S., Valero, M. A., & Bargues, M. D. (2009). Chapter 2. Fasciola, lymnaeids and human fascioliasis, with a global overview on disease transmission, epidemiology, evolutionary genetics, molecular epidemiology and control. Advances in parasitology, 69, 41–146. https://doi.org/10.1016/S0065-308X(09)69002-3
2. Beesley, N. J., Caminade, C., Charlier, J., Flynn, R. J., Hodgkinson, J. E., Martinez-Moreno, A., Martinez-Valladares, M., Perez, J., Rinaldi, L., & Williams, D. J. L. (2018). Fasciola and fasciolosis in ruminants in Europe: Identifying research needs. Transboundary and emerging diseases, 65 Suppl 1(Suppl 1), 199–216. https://doi.org/10.1111/tbed.12682
3. Girma, A., Teshome, K., Abdu, I., Genet, A., & Tamir, D. (2024). Prevalence and associated economic losses of bovine fasciolosis from postmortem inspection in municipal abattoirs in Ethiopia: A systematic review and meta-analysis. Veterinary and animal science, 24, 100360. https://doi.org/10.1016/j.vas.2024.100360

4. Lan, Z., Zhang, X. H., Xing, J. L., Zhang, A. H., Wang, H. R., Zhang, X. C., Gao, J. F., & Wang, C. R. (2024). Global prevalence of liver disease in human and domestic animals caused by Fasciola: A systematic review and meta-analysis. Journal of global health, 14, 04223. https://doi.org/10.7189/jogh.14.04223
5. Nyirenda, S. S., Sakala, M., Moonde, L., Kayesa, E., Fandamu, P., Banda, F., & Sinkala, Y. (2019). Prevalence of bovine fascioliasis and economic impact associated with liver condemnation in abattoirs in Mongu district of Zambia. BMC veterinary research, 15(1), 33. https://doi.org/10.1186/s12917-019-1777-0
6. Priddle, J., Mengersen, K., Swindells, D., Elliott, T., & Ralph, C. (2025). Carcass weight, meat quality and economic impact of liver fluke infection on cattle. Veterinary parasitology, regional studies and reports, 58, 101195. https://doi.org/10.1016/j.vprsr.2025.101195
7. González-Miguel, J., Becerro-Recio, D., Sotillo, J., Simón, F., & Siles-Lucas, M. (2020). Set up of an in vitro model to study early host-parasite interactions between newly excysted juveniles of *Fasciola hepatica* and host intestinal cells using a quantitative proteomics approach. Veterinary parasitology, 278, 109028. https://doi.org/10.1016/j.vetpar.2020.109028
8. Becerro-Recio, D., Serrat, J., López-García, M., Molina-Hernández, V., Pérez-Arévalo, J., Martínez-Moreno, Á., Sotillo, J., Simón, F., González-Miguel, J., & Siles-Lucas, M. (2022). Study of the migration of *Fasciola hepatica* juveniles across the intestinal barrier of the host by quantitative proteomics in an ex vivo model. PLoS neglected tropical diseases, 16(9), e0010766. https://doi.org/10.1371/journal.pntd.0010766
9. O'Kelly, E., Cwiklinski, K., De Marco Verissimo, C., Calvani, N. E. D., López Corrales, J., Jewhurst, H., Flaus, A., Lalor, R., Serrat, J., Dalton, J. P., & González-Miguel, J. (2024). Moonlighting on the *Fasciola hepatica* tegument: Enolase, a glycolytic enzyme, interacts with the extracellular matrix and fibrinolytic system of the host. PLoS neglected tropical diseases, 18(8), e0012069. https://doi.org/10.1371/journal.pntd.0012069
10. Serrat, J., Becerro-Recio, D., Torres-Valle, M., Simón, F., Valero, M. A., Bargues, M. D., Mas-Coma, S., Siles-Lucas, M., & González-Miguel, J. (2023). *Fasciola hepatica* juveniles interact with the host fibrinolytic system as a potential early-stage invasion mechanism. PLoS neglected tropical diseases, 17(4), e0010936. https://doi.org/10.1371/journal.pntd.0010936
11. Becerro-Recio, D., Serrat, J., López-García, M., Torres-Valle, M., Colina, F., Fernández, I. M., González-Miguel, J., & Siles-Lucas, M. (2023). Study of the cross-talk between *Fasciola hepatica* juveniles and the intestinal epithelial cells of the host by transcriptomics in an in vitro model. Veterinary parasitology, 320, 109981. https://doi.org/10.1016/j.vetpar.2023.109981
12. López-García, M., Cwiklinski, K., Becerro-Recio, D., Ruiz-Campillo, M. T., Molina-Hernández, V., Pérez-Arévalo, J., Martínez-Moreno, Á., González-Miguel, J., & Siles-Lucas, M. (2025). Deciphering the Proteomic Profile of the Parasite *Fasciola hepatica* After Initial Vertebrate Host Infection Reveals New Insights Into Its Early Stages. Molecular & cellular proteomics: MCP, 24(8), 101005. https://doi.org/10.1016/j.mcpro.2025.101005

13. Ambros, V., & Ruvkun, G. (2018). Recent Molecular Genetic Explorations of Caenorhabditis elegans MicroRNAs. Genetics, 209(3), 651–673. https://doi.org/10.1534/genetics.118.300291
14. Saliminejad, K., Khorram Khorshid, H. R., Soleymani Fard, S., & Ghaffari, S. H. (2019). An overview of microRNAs: Biology, functions, therapeutics, and analysis methods. Journal of cellular physiology, 234(5), 5451–5465. https://doi.org/10.1002/jcp.27486
15. Verma, P., Pandey, R. K., Prajapati, P., & Prajapati, V. K. (2016). Circulating MicroRNAs: Potential and Emerging Biomarkers for Diagnosis of Human Infectious Diseases. Frontiers in microbiology, 7, 1274. https://doi.org/10.3389/fmicb.2016.01274.
16. Correia, C. N., Nalpas, N. C., McLoughlin, K. E., Browne, J. A., Gordon, S. V., MacHugh, D. E., & Shaughnessy, R. G. (2017). Circulating microRNAs as Potential Biomarkers of Infectious Disease. Frontiers in immunology, 8, 118. https://doi.org/10.3389/fimmu.2017.00118.
17. Ojha, R., Nandani, R., Pandey, R. K., Mishra, A., & Prajapati, V. K. (2019). Emerging role of circulating microRNA in the diagnosis of human infectious diseases. Journal of cellular physiology, 234(2), 1030–1043. https://doi.org/10.1002/jcp.27127.
18. Turchinovich, A., Samatov, T. R., Tonevitsky, A. G., & Burwinkel, B. (2013). Circulating miRNAs: cell-cell communication function?. Frontiers in genetics, 4, 119. https://doi.org/10.3389/fgene.2013.00119.
19. Mori, M. A., Ludwig, R. G., Garcia-Martin, R., Brandão, B. B., & Kahn, C. R. (2019). Extracellular miRNAs: From Biomarkers to Mediators of Physiology and Disease. Cell metabolism, 30(4), 656–673. https://doi.org/10.1016/j.cmet.2019.07.011.
20. Katayama, E. S., Hue, J. J., Loftus, A. W., Ali, S. A., Graor, H. J., Rothermel, L. D., Londin, E., Zarei, M., & Winter, J. M. (2025). Stability of microRNAs in serum and plasma reveal promise as a circulating biomarker. Non-coding RNA research, 15, 132–141. https://doi.org/10.1016/j.ncrna.2025.08.001.
21. Rojas-Pirela, M., Andrade-Alviárez, D., Quiñones, W., Rojas, M. V., Castillo, C., Liempi, A., Medina, L., Guerrero-Muñoz, J., Fernández-Moya, A., Ortega, Y. A., Araneda, S., Maya, J. D., & Kemmerling, U. (2022). microRNAs: Critical Players during Helminth Infections. Microorganisms, 11(1), 61. https://doi.org/10.3390/microorganisms11010061.
22. Mu, Y., McManus, D. P., Gordon, C. A., & Cai, P. (2021). Parasitic Helminth-Derived microRNAs and Extracellular Vesicle Cargos as Biomarkers for Helminthic Infections. Frontiers in cellular and infection microbiology, 11, 708952. https://doi.org/10.3389/fcimb.2021.708952.
23. Pinheiro, A. A. S., Torrecilhas, A. C., Souza, B. S. F., Cruz, F. F., Guedes, H. L. M., Ramos, T. D., Lopes-Pacheco, M., Caruso-Neves, C., & Rocco, P. R. M. (2024). Potential of extracellular vesicles in the pathogenesis, diagnosis and therapy for parasitic diseases. Journal of extracellular vesicles, 13(8), e12496. https://doi.org/10.1002/jev2.12496.
24. Barrero-Torres, D. M., Herrera-Torres, G., Pérez, J., Martínez-Moreno, Á., Martínez-Moreno, F. J., Flores-Velázquez, L. M., Buffoni, L., Rufino-Moya, P. J., Ruiz-Campillo, M. T., & Molina-Hernández, V. (2024). Unraveling the microRNAs Involved in Fasciolosis: Master Regulators of the Host-Parasite

Crosstalk. International journal of molecular sciences, 26(1), 204. https://doi.org/10.3390/ijms26010204.

25. Hansen, E. P., Fromm, B., Andersen, S. D., Marcilla, A., Andersen, K. L., Borup, A., Williams, A. R., Jex, A. R., Gasser, R. B., Young, N. D., Hall, R. S., Stensballe, A., Ovchinnikov, V., Yan, Y., Fredholm, M., Thamsborg, S. M., & Nejsum, P. (2019). Exploration of extracellular vesicles from Ascaris suum provides evidence of parasite-host cross talk. Journal of extracellular vesicles, 8(1), 1578116. https://doi.org/10.1080/20013078.2019.1578116.
26. Li, S., Giri, B. R., Liu, J., He, X., Cai, P., Jing, Z., & Cheng, G. (2022). Characterization of MicroRNA Cargo of Extracellular Vesicles Isolated From the Plasma of Schistosoma japonicum-Infected Mice. Frontiers in cellular and infection microbiology, 12, 803242. https://doi.org/10.3389/fcimb.2022.803242.
27. Ullah, H., Tian, Y., Arbab, S., Li, K., Khan, M. I. U., Rahman, S. U., Qadeer, A., Muhammad, N., Suleman, & Hassan, I. U. (2022). Circulatory microRNAs in helminthiases: Potent as diagnostics biomarker, its potential role and limitations. Frontiers in veterinary science, 9, 1018872. https://doi.org/10.3389/fvets.2022.1018872.
28. Witwer K. W. (2015). Circulating microRNA biomarker studies: pitfalls and potential solutions. Clinical chemistry, 61(1), 56–63. https://doi.org/10.1373/clinchem.2014.221341.
29. Faraldi, M., Gomarasca, M., Banfi, G., & Lombardi, G. (2019). Free Circulating miRNAs Measurement in Clinical Settings: The Still Unsolved Issue of the Normalization. Advances in clinical chemistry, 87, 113–139. https://doi.org/10.1016/bs.acc.2018.07.003.
30. Ruiz-Campillo, M. T., Barrero-Torres, D. M., Abril, N., Pérez, J., Zafra, R., Buffoni, L., Martínez-Moreno, Á., Martínez-Moreno, F. J., & Molina-Hernández, V. (2023). *Fasciola hepatica* primoinfections and reinfections in sheep drive distinct Th1/Th2/Treg immune responses in liver and hepatic lymph node at early and late stages. Veterinary research, 54(1), 2. https://doi.org/10.1186/s13567-022-01129-7.
31. Barrero-Torres, D. M., Herrera-Torres, G., Huertas-Abril, P. V., Abril, N., Pérez, J., Rufino-Moya, P. J., Suárez-Cárdenas, J. M., Zaldívar-López, S., Martínez-Moreno, Á., Ruiz-Campillo, M. T., & Molina-Hernández, V. (2026). Identification of stable miRNA references for RT-qPCR normalization in ovine fasciolosis. BMC genomics, 27(1), 579. https://doi.org/10.1186/s12864-026-12928-z
32. Kirschner, M. B., Kao, S. C., Edelman, J. J., Armstrong, N. J., Vallely, M. P., van Zandwijk, N., & Reid, G. (2011). Haemolysis during sample preparation alters microRNA content of plasma. PloS one, 6(9), e24145. https://doi.org/10.1371/journal.pone.0024145.
33. Blondal, T., Jensby Nielsen, S., Baker, A., Andreasen, D., Mouritzen, P., Wrang Teilum, M., & Dahlsveen, I. K. (2013). Assessing sample and miRNA profile quality in serum and plasma or other biofluids. Methods (San Diego, Calif.), 59(1), S1–S6. https://doi.org/10.1016/j.ymeth.2012.09.015.
34. Bustin, S. A., Benes, V., Garson, J. A., Hellemans, J., Huggett, J., Kubista, M., Mueller, R., Nolan, T., Pfaffl, M. W., Shipley, G. L., Vandesompele, J., & Wittwer, C. T. (2009). The MIQE guidelines: minimum information for publication of quantitative real-time PCR experiments. Clinical chemistry, 55(4), 611–622. https://doi.org/10.1373/clinchem.2008.112797.

35. Bustin, S. A., Ruijter, J. M., van den Hoff, M. J. B., Kubista, M., Pfaffl, M. W., Shipley, G. L., Tran, N., Rödiger, S., Untergasser, A., Mueller, R., Nolan, T., Milavec, M., Burns, M. J., Huggett, J. F., Vandesompele, J., & Wittwer, C. T. (2025). MIQE 2.0: Revision of the Minimum Information for Publication of Quantitative Real-Time PCR Experiments Guidelines. Clinical chemistry, 71(6), 634–651. https://doi.org/10.1093/clinchem/hvaf043.
36. Bezman, N. A., Cedars, E., Steiner, D. F., Blelloch, R., Hesslein, D. G., & Lanier, L. L. (2010). Distinct requirements of microRNAs in NK cell activation, survival, and function. Journal of immunology (Baltimore, Md.: 1950), 185(7), 3835–3846. https://doi.org/10.4049/jimmunol.1000980.
37. Bandiera, S., Pfeffer, S., Baumert, T. F., & Zeisel, M. B. (2015). miR-122–a key factor and therapeutic target in liver disease. Journal of hepatology, 62(2), 448–457. https://doi.org/10.1016/j.jhep.2014.10.004.
38. Sheedy F. J. (2015). Turning 21: Induction of miR-21 as a Key Switch in the Inflammatory Response. Frontiers in immunology, 6, 19. https://doi.org/10.3389/fimmu.2015.00019.
39. González-Martin, A., Adams, B. D., Lai, M., Shepherd, J., Salvador-Bernaldez, M., Salvador, J. M., Lu, J., Nemazee, D., & Xiao, C. (2016). The microRNA miR-148a functions as a critical regulator of B cell tolerance and autoimmunity. Nature immunology, 17(4), 433–440. https://doi.org/10.1038/ni.3385.
40. Chowdhury, S., Ricafrente, A., Cwiklinski, K., Sais, D., Dalton, J. P., Tran, N., & Donnelly, S. (2024). Exploring the utility of circulating miRNAs as diagnostic biomarkers of fasciolosis. Scientific reports, 14(1), 7431. https://doi.org/10.1038/s41598-024-57704-9.
41. Roush, S., & Slack, F. J. (2008). The let-7 family of microRNAs. Trends in cell biology, 18(10), 505–516. https://doi.org/10.1016/j.tcb.2008.07.007.
42. Chen, X., Ba, Y., Ma, L., Cai, X., Yin, Y., Wang, K., Guo, J., Zhang, Y., Chen, J.,Guo, X., Li, Q., Li, X., Wang, W., Zhang, Y., Wang, J., Jiang, X., Xiang, Y., Xu,C., Zheng, P., Zhang, J., … Zhang, C. Y. (2008). Characterization of microRNAs in serum: a novel class of biomarkers for diagnosis of cancer and other diseases. Cell research, 18(10), 997–1006. https://doi.org/10.1038/cr.2008.282.
43. Li, Q. J., Chau, J., Ebert, P. J., Sylvester, G., Min, H., Liu, G., Braich, R., Manoharan, M., Soutschek, J., Skare, P., Klein, L. O., Davis, M. M., & Chen, C. Z. (2007). miR-181a is an intrinsic modulator of T cell sensitivity and selection. Cell, 129(1), 147–161. https://doi.org/10.1016/j.cell.2007.03.008.
44. Kriegel, A. J., Liu, Y., Fang, Y., Ding, X., & Liang, M. (2012). The miR-29 family: genomics, cell biology, and relevance to renal and cardiovascular injury. Physiological genomics, 44(4), 237–244. https://doi.org/10.1152/physiolgenomics.00141.2011
45. Schwarzenbach, H., Nishida, N., Calin, G. A., & Pantel, K. (2014). Clinical relevance of circulating cell-free microRNAs in cancer. Nature reviews. Clinical oncology, 11(3), 145–156. https://doi.org/10.1038/nrclinonc.2014.5
46. Sun, J., Yan, P., Chen, Y., Chen, Y., Yang, J., Xu, G., Mao, H., & Qiu, Y. (2015). MicroRNA-26b inhibits cell proliferation and cytokine secretion in human RASF cells via the Wnt/GSK-3β/β-catenin pathway. Diagnostic pathology, 10, 72. https://doi.org/10.1186/s13000-015-0309-x

47. Ban, E., & Song, E. J. (2022). Considerations and Suggestions for the Reliable Analysis of miRNA in Plasma Using RT-qPCR. Genes, 13(2), 328. https://doi.org/10.3390/genes13020328.
48. Kroh, E. M., Parkin, R. K., Mitchell, P. S., & Tewari, M. (2010). Analysis of circulating microRNA biomarkers in plasma and serum using quantitative reverse transcription-PCR (RT-qPCR). Methods (San Diego, Calif.), 50(4), 298–301. https://doi.org/10.1016/j.ymeth.2010.01.032.
49. Wen, J., & Friedman, J. R. (2012). miR-122 regulates hepatic lipid metabolism and tumor suppression. The Journal of clinical investigation, 122(8), 2773–2776. https://doi.org/10.1172/JCI63966.
50. Bala, S., Petrasek, J., Mundkur, S., Catalano, D., Levin, I., Ward, J., Alao, H., Kodys, K., & Szabo, G. (2012). Circulating microRNAs in exosomes indicate hepatocyte injury and inflammation in alcoholic, drug-induced, and inflammatory liver diseases. Hepatology, 56(5), 1946–1957. https://doi.org/10.1002/hep.25873.
51. Vliegenthart, A. D. B., Berends, C., Potter, C. M. J., Kersaudy-Kerhoas, M., & Dear, J. W. (2017). MicroRNA-122 can be measured in capillary blood which facilitates point-of-care testing for drug-induced liver injury. British Journal of Clinical Pharmacology, 83(9), 2027–2033. https://doi.org/10.1111/bcp.13282.
52. Hörauf, J. A., Singh, A., Voth, M., Moheimani, H., Schindler, C. R., Relja, B., Leppik, L., Marzi, I., & Henrich, D. (2025). Limited Diagnostic Value of miRNAs in Early Trauma-Induced Liver Injury: Only miRNA-122 Emerges as a Late-Phase Marker. Diagnostics (Basel, Switzerland), 15(2), 179. https://doi.org/10.3390/diagnostics15020179.
53. Lalor, R., Cwiklinski, K., Calvani, N. E. D., Dorey, A., Hamon, S., Corrales, J. L., Dalton, J. P., & De Marco Verissimo, C. (2021). Pathogenicity and virulence of the liver flukes *Fasciola hepatica*and *Fasciola gigantica*that cause the zoonosis Fasciolosis. Virulence, 12(1), 2839–2867. https://doi.org/10.1080/21505594.2021.1996520.
54. Cwiklinski, K., Jewhurst, H., McVeigh, P., Barbour, T., Maule, A. G., Tort, J., O'Neill, S. M., Robinson, M. W., Donnelly, S., & Dalton, J. P. (2018). Infection by the Helminth Parasite *Fasciola hepatica* Requires Rapid Regulation of Metabolic, Virulence, and Invasive Factors to Adjust to Its Mammalian Host. Molecular & cellular proteomics: MCP, 17(4), 792–809. https://doi.org/10.1074/mcp.RA117.000445.
55. Alvarez Rojas, C. A., Scheerlinck, J. P., Ansell, B. R., Hall, R. S., Gasser, R. B., & Jex, A. R. (2016). Time-Course Study of the Transcriptome of Peripheral Blood Mononuclear Cells (PBMCs) from Sheep Infected with *Fasciola hepatica*. PloS one, 11(7), e0159194. https://doi.org/10.1371/journal.pone.0159194.
56. Vogt, J., Sheinson, D., Katavolos, P., Irimagawa, H., Tseng, M., Alatsis, K. R., & Proctor, W. R. (2019). Variance component analysis of circulating miR-122 in serum from healthy human volunteers. PloS one, 14(7), e0220406. https://doi.org/10.1371/journal.pone.0220406.
57. Zhi, Y., Hu, B., Tian, S., Bai, Y., & Chen, X. (2025). Screening and validation of key microRNAs regulating muscle development in Hanper sheep. PloS one, 20(6), e0325054. https://doi.org/10.1371/journal.pone.0325054.

58. Paluschinski, M., Schira-Heinen, J., Pellegrino, R., Heij, L. R., Bednarsch, J., Neumann, U. P., Longerich, T., Stuehler, K., Luedde, T., & Castoldi, M. (2023). Uncovering Novel Roles of miR-122 in the Pathophysiology of the Liver: Potential Interaction with NRF1 and E2F4 Signaling. Cancers, 15(16), 4129. https://doi.org/10.3390/cancers15164129.
59. Zhou, B., Wang, S., Mayr, C., Bartel, D. P., & Lodish, H. F. (2007). miR-150, a microRNA expressed in mature B and T cells, blocks early B cell development when expressed prematurely. Proceedings of the National Academy of Sciences of the United States of America, 104(17), 7080–7085. https://doi.org/10.1073/pnas.0702409104.
60. Sang, W., Wang, Y., Zhang, C., Zhang, D., Sun, C., Niu, M., Zhang, Z., Wei, X., Pan, B., Chen, W., Yan, D., Zeng, L., Loughran, T. P., Jr, & Xu, K. (2016). MiR-150 impairs inflammatory cytokine production by targeting ARRB-2 after blocking CD28/B7 costimulatory pathway. Immunology letters, 172, 1–10. https://doi.org/10.1016/j.imlet.2015.11.001.
61. Karginov, T. A., Ménoret, A., Karlinsey, K., Agliano, F., Zhou, B., & Vella, A. T. (2023). Antigen-specific downregulation of miR-150 in CD4 T cells promotes cell survival. Frontiers in Immunology, 14, 1102403. https://doi.org/10.3389/fimmu.2023.1102403.
62. Niedziela, D. A., Naranjo-Lucena, A., Molina-Hernández, V., Browne, J. A., Martínez-Moreno, Á., Pérez, J., MacHugh, D. E., & Mulcahy, G. (2021). Timing of Transcriptomic Peripheral Blood Mononuclear Cell Responses of Sheep to *Fasciola hepatica* Infection Differs from Those of Cattle, Reflecting Different Disease Phenotypes. Frontiers in immunology, 12, 729217. https://doi.org/10.3389/fimmu.2021.729217.
63. Shi, W., He, J. J., Mei, X. F., Lu, K. J., Zeng, Z. X., Zhang, Y. Y., Sheng, Z. A., Elsheikha, H. M., Huang, W. Y., & Zhu, X. Q. (2020). Dysregulation of hepatic microRNA expression in C57BL/6 mice affected by excretory-secretory products of *Fasciola gigantica*. PLoS neglected tropical diseases, 14(12), e0008951. https://doi.org/10.1371/journal.pntd.0008951.
64. Bernstein, D. L., Jiang, X., & Rom, S. (2021). let-7 microRNAs: Their Role in Cerebral and Cardiovascular Diseases, Inflammation, Cancer, and Their Regulation. Biomedicines, 9(6), 606. https://doi.org/10.3390/biomedicines9060606.
65. Zhong, H., Guan, G., & Jin, Y. (2024). Roles of helminth extracellular vesicle-derived let-7 in host-parasite crosstalk. Frontiers in immunology, 15, 1449495. https://doi.org/10.3389/fimmu.2024.1449495
66. Haftmann, C., Stittrich, A.-B., Zimmermann, J., Fang, Z., Hradilkova, K., Bardua, M., Westendorf, K., Heinz, G.A., Riedel, R., Siede, J., Lehmann, K., Weinberger, E.E., Zimmel, D., Lauer, U., Häupl, T., Sieper, J., Backhaus, M., Neumann, C., Hoffmann, U., Porstner, M., Chen, W., Grün, J.R., Baumgrass, R., Matz, M., Löhning, M., Scheffold, A., Wittmann, J., Chang, H.-D., Rajewsky, N., Jäck, H.-M., Radbruch, A. & Mashreghi, M.-F. (2015). miR-148a is upregulated by Twist1 and T-bet and promotes Th1-cell survival by regulating the proapoptotic gene Bim. European Journal of Immunology, 45(4), 1192–1205. https://doi.org/10.1002/eji.201444633.

67. Ruiz-Campillo, M. T., Molina Hernández, V., Escamilla, A., Stevenson, M., Perez, J., Martinez-Moreno, A., Donnelly, S., Dalton, J. P., & Cwiklinski, K. (2017). Immune signatures of pathogenesis in the peritoneal compartment during early infection of sheep with *Fasciola hepatica*. Scientific reports, 7(1), 2782. https://doi.org/10.1038/s41598-017-03094-0.

68. Pérez-Caballero, R., Javier Martínez-Moreno, F., Zafra, R., Molina-Hernández, V., Pacheco, I. L., Ruiz-Campillo, M.T., Escamilla, A., Pérez, J., Martínez-Moreno, Á., & Buffoni, L. (2018). Comparative dynamics of peritoneal cell immunophenotypes in sheep during the early and late stages of the infection with *Fasciola hepatica* by flow cytometric analysis. Parasites & vectors, 11(1), 640. https://doi.org/10.1186/s13071-018-3250-5.

69. Lu, T. X., Hartner, J., Lim, E. J., Fabry, V., Mingler, M. K., Cole, E. T., Orkin, S. H., Aronow, B. J., & Rothenberg, M. E. (2011). MicroRNA-21 limits in vivo immune response-mediated activation of the IL-12/IFN-gamma pathway, Th1 polarization, and the severity of delayed-type hypersensitivity. Journal of immunology (Baltimore, Md.: 1950), 187(6), 3362–3373. https://doi.org/10.4049/jimmunol.1101235

70. Wang, Z., Brandt, S., Medeiros, A., Wang, S., Wu, H., Dent, A., & Serezani, C. H. (2015). MicroRNA 21 is a homeostatic regulator of macrophage polarization and prevents prostaglandin E2-mediated M2 generation. PloS one, 10(2), e0115855. https://doi.org/10.1371/journal.pone.0115855

71. Anada, N., Nakayama, Y., Takeshita, J., Kageyama, K., Sakamoto, H., Kamibayashi, T., & Nakajima, Y. (2024). Role of MicroRNA-21 in Regulating Intracellular Pathways Associated with Phagocytosis in Human Macrophages: An In Vitro Study. Cureus, 16(7), e63736. https://doi.org/10.7759/cureus.63736

72. Naranjo-Lucena, A., Correia, C. N., Molina-Hernández, V., Martínez-Moreno, Á., Browne, J. A., Pérez, J., MacHugh, D. E., & Mulcahy, G. (2021). Transcriptomic analysis of ovine hepatic lymph node following *Fasciola hepatica* infection -inhibition of NK cell and IgE-mediated signaling. Frontiers in Immunology, 12, 687579. https://doi.org/10.3389/fimmu.2021.687579

73. Lykken, E. A., & Li, Q. J. (2016). The MicroRNA miR-191 Supports T Cell Survival Following Common γ Chain Signaling. The Journal of biological chemistry,291(45), 23532–23544. https://doi.org/10.1074/jbc.M116.741264.

74. Pan, W., Wang, L., Zhang, X. F., Zhang, H., Zhang, J., Wang, G., Xu, P., Zhang, Y., Hu, P., Zhang, X. D., Du, R. L., & Wang, H. (2019). Hypoxia-induced microRNA-191 contributes to hepatic ischemia/reperfusion injury through the ZONAB/Cyclin D1 axis. Cell death and differentiation, 26(2), 291–305. https://doi.org/10.1038/s41418-018-0120-9.

75. Roderburg, C., Urban, G. W., Bettermann, K., Vucur, M., Zimmermann, H., Schmidt, S., Janssen, J., Koppe, C., Knolle, P., Castoldi, M., Tacke, F., Trautwein, C., & Luedde, T. (2011). Micro-RNA profiling reveals a role for miR-29 in human and murine liver fibrosis. Hepatology (Baltimore, Md.), 53(1), 209–218. https://doi.org/10.1002/hep.23922.

76. Yu, X., Elfimova, N., Müller, M., Bachurski, D., Koitzsch, U., Drebber, U., Mahabir, E., Hansen, H. P., Friedman, S. L., Klein, S., Dienes, H. P., Hösel, M., Buettner, R., Trebicka, J., Kondylis, V., Mannaerts, I.,

& Odenthal, M. (2022). Autophagy-Related Activation of Hepatic Stellate Cells Reduces Cellular miR-29a by Promoting Its Vesicular Secretion. Cellular and molecular gastroenterology and hepatology, 13(6), 1701–1716. https://doi.org/10.1016/j.jcmgh.2022.02.013.

77. Lin, Y. C., Wang, F. S., Yang, Y. L., Chuang, Y. T., & Huang, Y. H. (2018). MicroRNA-29a mitigation of toll-like receptor 2 and 4 signaling and alleviation of obstructive jaundice-induced fibrosis in mice. Biochemical and biophysical research communications, 496(3), 880–886. https://doi.org/10.1016/j.bbrc.2018.01.132.
78. Flynn, R. J., & Mulcahy, G. (2008). The roles of IL-10 and TGF-beta in controlling IL-4 and IFN-gamma production during experimental *Fasciola hepatica* infection. International journal for parasitology, 38(14), 1673–1680. https://doi.org/10.1016/j.ijpara.2008.05.008.
79. Cwiklinski, K., de la Torre-Escudero, E., Trelis, M., Bernal, D., Dufresne, P. J., Brennan, G. P., O'Neill, S., Tort, J., Paterson, S., Marcilla, A., Dalton, J. P., & Robinson, M. W. (2015). The extracellular vesicles of the helminth pathogen, *Fasciola hepatica*: Biogenesis pathways and cargo molecules involved in parasite pathogenesis. Molecular & Cellular Proteomics, 14(12), 3258–3273. https://doi.org/10.1074/mcp.M115.053934.
80. Heegaard, N. H. H., Carlsen, A. L., Skovgaard, K., & Heegaard, P. M. H. (2015). Circulating Extracellular microRNA in Systemic Autoimmunity. Experientia supplementum (2012), 106, 171–195. https://doi.org/10.1007/978-3-0348-0955-9_8
81. Boukouris, S., & Mathivanan, S. (2015). Exosomes in bodily fluids are a highly stable resource of disease biomarkers. Proteomics. Clinical applications, 9(3–4), 358–367. https://doi.org/10.1002/prca.201400114.
82. Ljungström, M., & Oltra, E. (2025). Methods for Extracellular Vesicle Isolation: Relevance for Encapsulated miRNAs in Disease Diagnosis and Treatment. Genes, 16(3), 330. https://doi.org/10.3390/genes16030330.

Figures

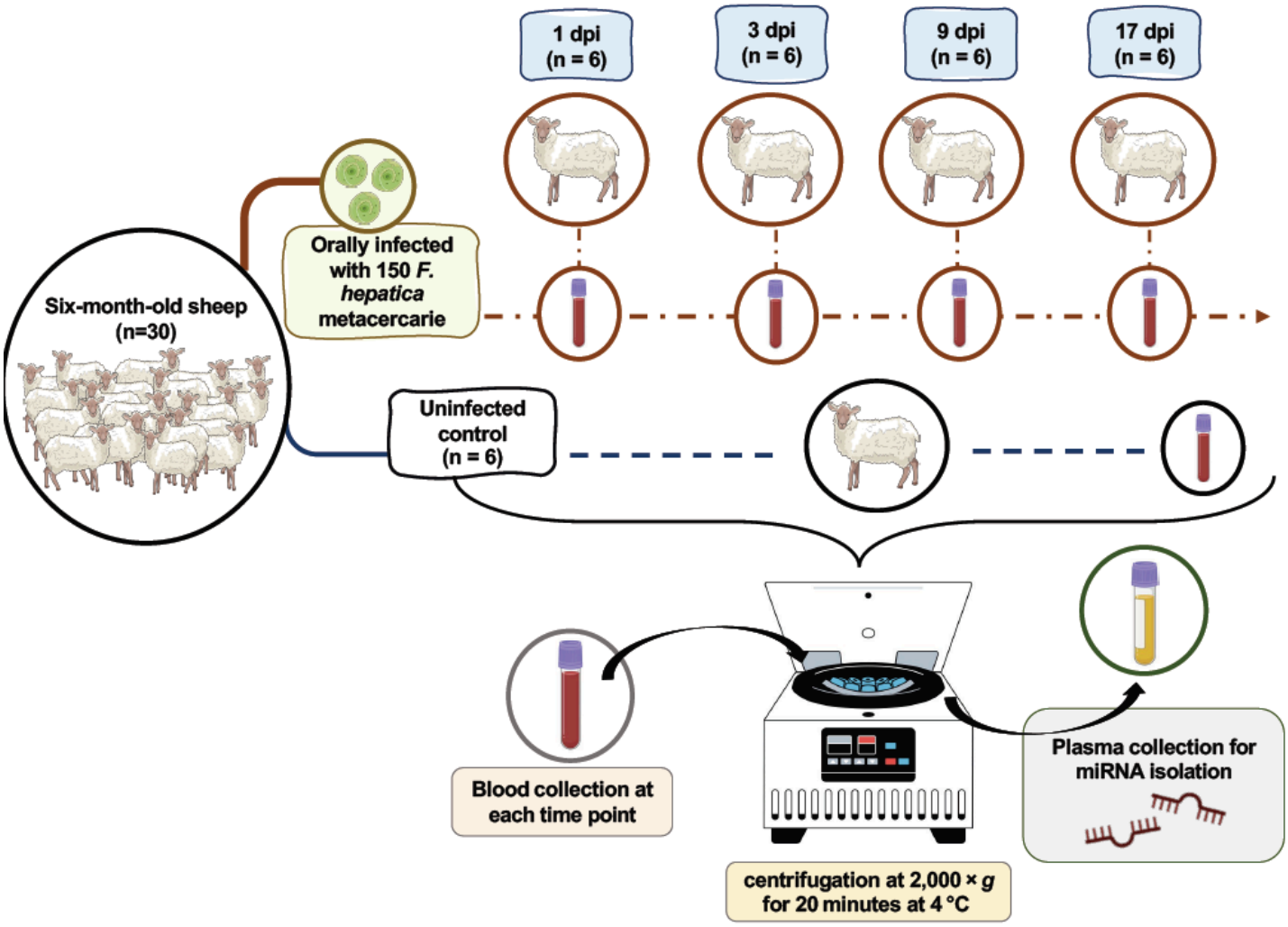


Figure 1

Overview of the experimental design. Sheep were assigned to either control or infection groups. At each scheduled sampling point, blood specimens were obtained and processed to recover plasma by centrifugation.

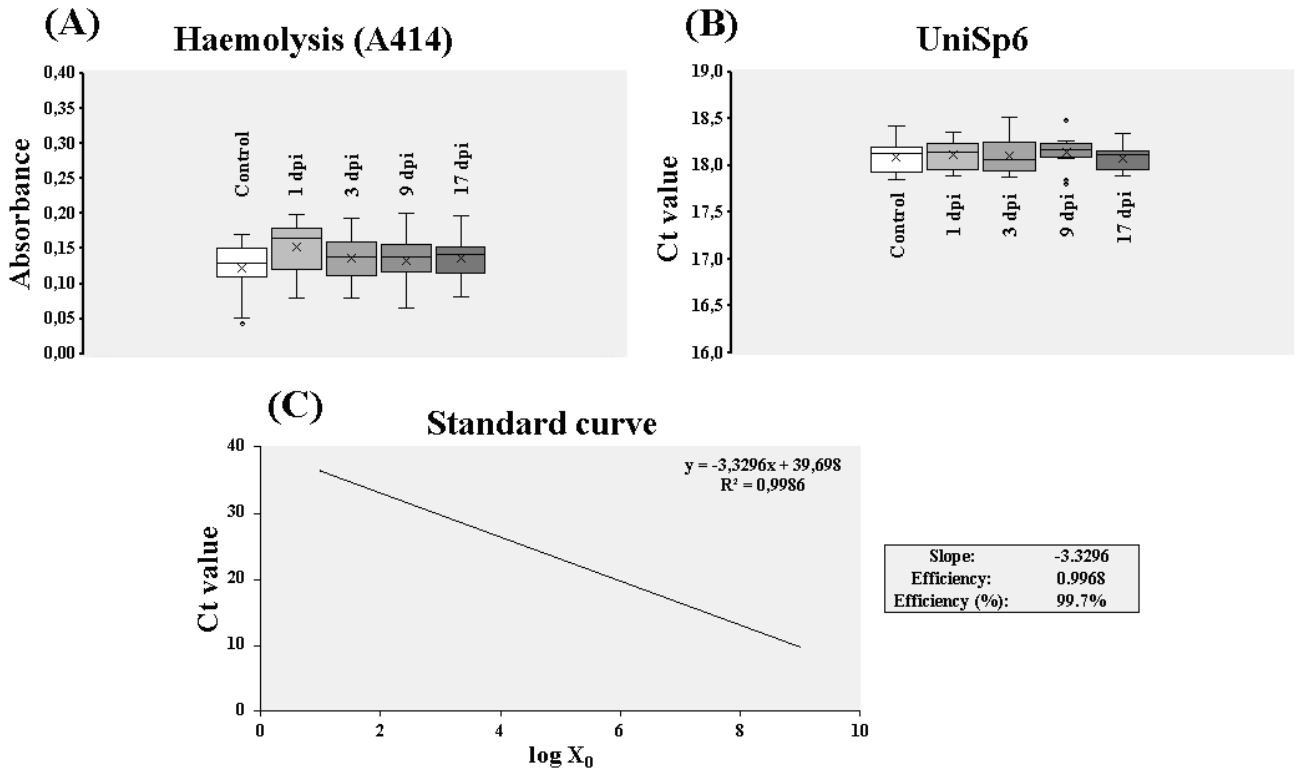


Figure 2

Analytical validation of the absolute RT-qPCR workflow for circulating miRNA quantification. **(A)** Spectrophotometric assessment of plasma haemolysis based on absorbance at 414 nm (A_{414}). All samples remained below the 0.20 threshold associated with significant haemolysis-related bias. Group mean ± SEM values were: control (0.12 ± 0.02); 1 dpi (0.15 ± 0.02); 3 dpi (0.14 ± 0.02); 9 dpi (0.13 ± 0.02); and 17 dpi (0.14 ± 0.01). **(B)** Ct values obtained for the UniSp6 synthetic spike-in control demonstrating high consistency of reverse transcription efficiency across experimental groups. **(C)** Standard curve generated from serial dilutions of synthetic cel-miR-39 RNA used for absolute quantification. The assay showed excellent linearity across the dynamic range analysed (R^2= 0.9986) with an amplification efficiency of approximately 99.7%. Detailed haemolysis measurements and UniSp6 amplification data corresponding to the biological samples and experimental infection model analysed in the present study were previously reported as supplementary material in Barrero-Torres et al. 2026 [31] (Table S4 and S5, respectively).

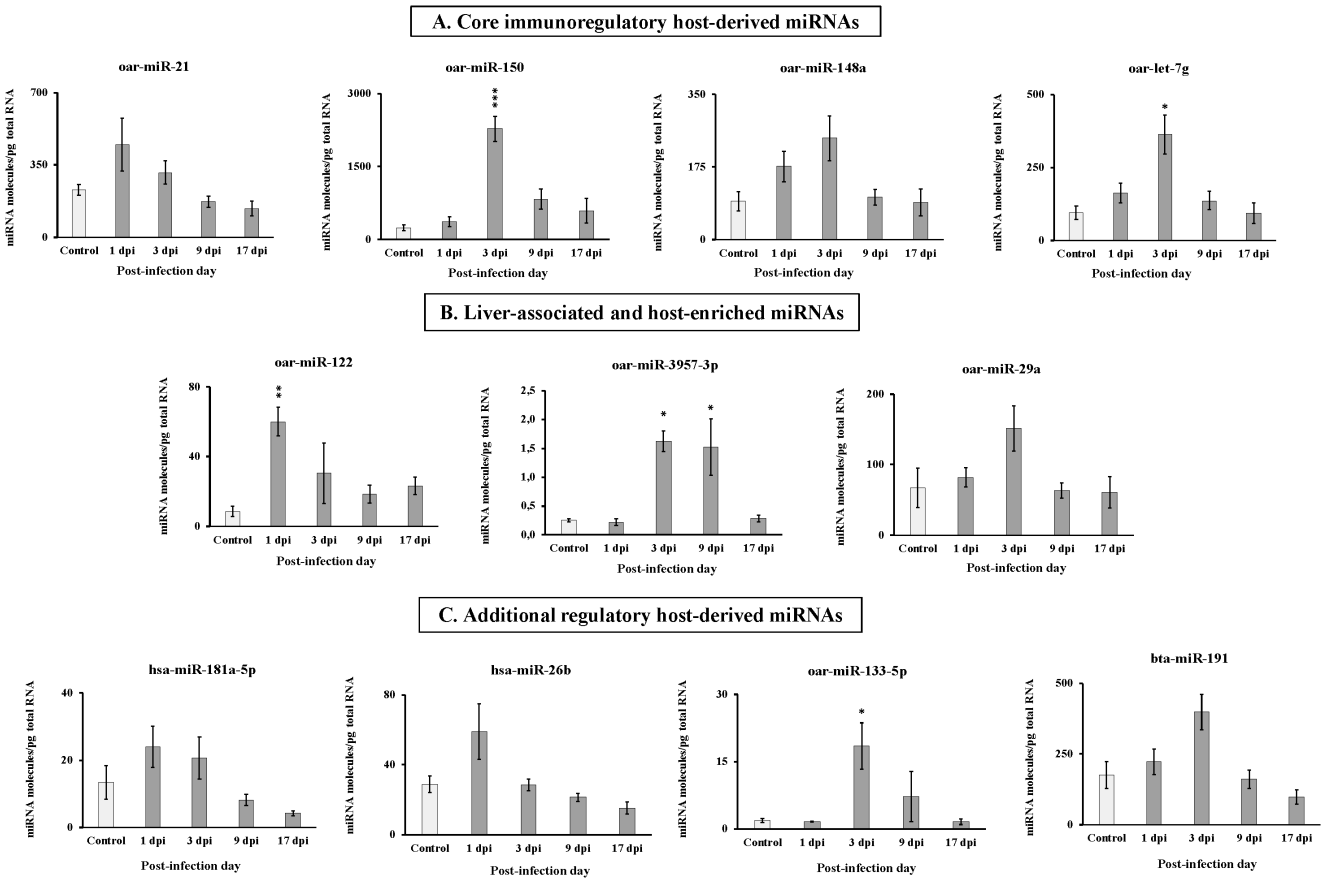
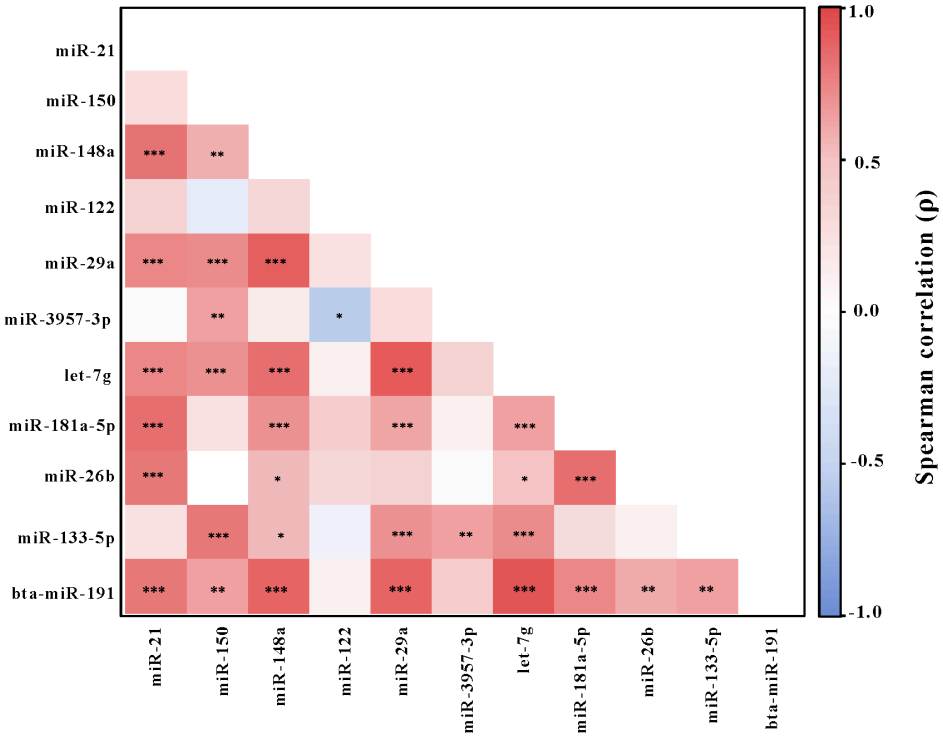


Figure 3

Temporal dynamics of core host-derived circulating miRNAs during early experimental *F. hepatica* infection. Absolute abundance profiles of miRNAs quantified in plasma samples from uninfected control sheep and experimentally infected animals at 1, 3, 9, and 17 days post-infection (dpi). miRNAs were classified into three categories according to their functional relevance and/or tissue association: **(A)** central host-derived immunoregulatory miRNAs, including oar-miR-21, oar-miR-150, oar-miR-148a, and oar-let-7g; **(B)**liver-associated, host-enriched miRNAs, including oar-miR-122, oar-miR-3957-3p, and oar-miR-29a; and **(C)** additional host-derived regulatory miRNAs, including hsa-miR-181a-5p, hsa-miR-26b, oar-miR-133-5p, and bta-miR-191. Absolute expression levels are expressed as miRNA molecules per pg of total RNA. Data are presented as mean ± SEM. Statistical comparisons were performed using the Kruskal-Wallis test followed by Dunn's post hoc multiple-comparisons test with Benjamini-Hochberg correction. Significant differences relative to uninfected controls are indicated as follows: ***adjusted *P* < 0.05, ****adjusted *P* < 0.01, and *****adjusted *P*< 0.001.

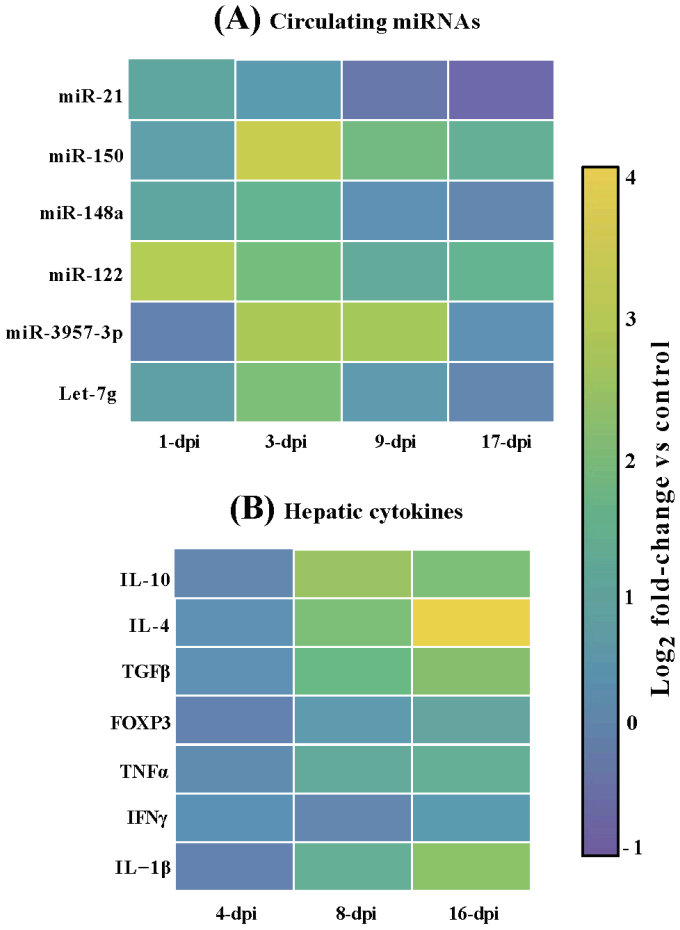


Top significant positive and negative correlations

Circulating miRNAs	ρ	Adjusted p
Positive correlations		
let-7g vs bta-miR-191	0.92	<0.001
miR-29a vs let-7g	0.92	<0.001
miR-148a vs miR-29a	0.90	<0.001
miR-29a vs bta-miR-191	0.87	<0.001
miR-148a vs bta-miR-191	0.87	<0.001
Negative correlations		
miR-122 vs miR-3957-3p	-0.54	<0.005

Figure 4

Pairwise associations among circulating miRNAs during early experimental fasciolosis. Spearman correlation heatmap illustrating pairwise associations between host-derived circulating miRNAs quantified in plasma samples from experimentally infected sheep during the early stages of *F. hepatica*infection (*n* = 24). Spearman correlation analyses were performed using absolute circulating miRNA abundance, expressed as transcript molecules per pg of total RNA. Positive associations are shown in red and negative associations in blue, with colour intensity proportional to the magnitude of Spearman's rank correlation coefficient (ρ). Statistically significant associations following Benjamini-Hochberg false discovery rate correction are indicated by asterisks **(*adjusted*P* < 0.05, adjusted *P* < 0.01, and ***adjusted *P* < 0.001)**. The accompanying summary table highlights the strongest significant positive and negative associations identified within the circulating miRNA dataset.



(C) Temporal association network

Circulating miRNAs	Hepatic mediator	Association module	Interpretation note
miR-21	IL-10 Liver TGFβ Liver	Immunoregulatory/Treg-associated temporal association Immunoregulatory/TGFβ-associated temporal association	Parallel regularoty response; no formal individual-level correlation
miR-150	IL-10 Lier TGFβ Liver	Early systemic immunoregulatory association	Parallel temporal modulation; no formal individual-level correlation
let-7g	TGFβ Liver FOXP3 Liver	Regulatory/homeostatic temporal association	
miR-148a	FOXP3 Liver	Regulatory/homeostatic temporal association	
miR-122	TNFα Liver IL-1β Liver	Hepatic perturbation/inflammatory temporal association	Temporal proximity but no formal individual-level correlation
miR-3957-3p	IL-4 Liver	Ovine-specific/Th2-associated temporal association	Parallel temporal modulation; no formal individual-level correlation

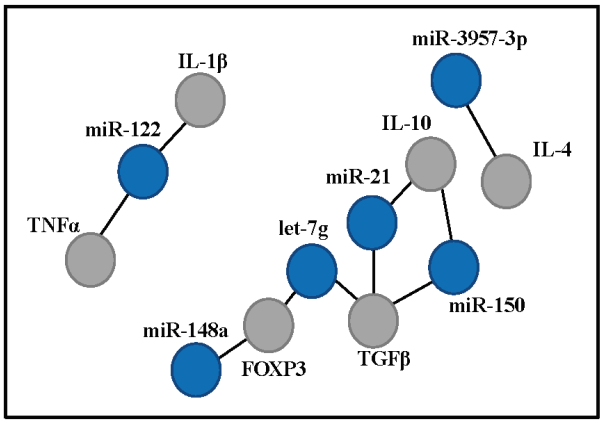


Figure 5

Comparative temporal dynamics of circulating miRNA abundance and hepatic cytokine gene expression during experimental *F. hepatica* infection. **(A)** Temporal dynamics of circulating miRNAs during early experimental *F. hepatica* infection. Heatmap values represent $\log_2$ fold changes in infected animals at 1, 3, 9, and 17 days post-infection (dpi) relative to uninfected controls. Warmer colours indicate higher circulating miRNA abundance relative to controls, whereas cooler colours indicate lower relative abundance. **(B)** Temporal dynamics of hepatic cytokine gene expression during experimental *F. hepatica* infection. Heatmap values represent $\log_2$ fold changes in infected animals at 4, 8, and 16 dpi relative to uninfected controls. Hepatic transcriptional data were obtained from a previously published independent study by Ruiz-Campillo et al. (2023) [30], conducted under comparable experimental infection conditions using a separate cohort of animals. **(C)** Conceptual schematic illustrating the partially overlapping temporal patterns observed between circulating extracellular miRNAs and previously reported hepatic cytokine transcriptional responses during experimental fasciolosis. This schematic is intended solely as a descriptive framework for visual comparison and does not imply experimentally validated functional

interactions or direct molecular correlations between circulating miRNAs and hepatic cytokine expression.

Supplementary Files

This is a list of supplementary files associated with this preprint. Click to download.

- SupplementaryFigures.pdf
- AccessibilityDescriptionsSubmissionForm.xlsx
- SupplementaryInformation.xlsx